



US Army Corps  
of Engineers

TECHNICAL REPORT ITL-90-6

# USER'S GUIDE FOR THE INCREMENTAL CONSTRUCTION SOIL-STRUCTURE INTERACTION PROGRAM SOILSTRUCT

by

R. M. Ebeling

Information Technology Laboratory

J. F. Peters

Geotechnical Laboratory

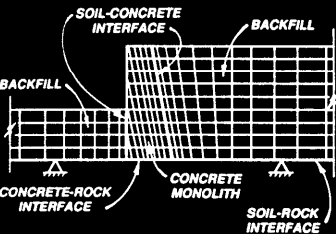
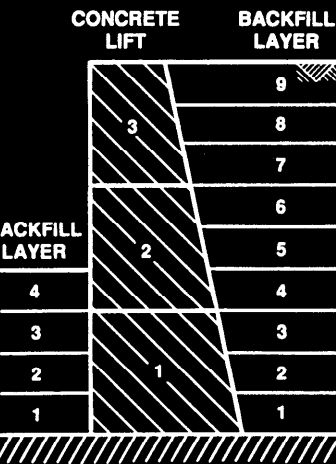
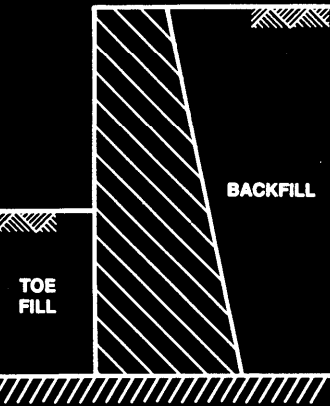
DEPARTMENT OF THE ARMY

Waterways Experiment Station, Corps of Engineers  
3909 Halls Ferry Road, Vicksburg, Mississippi 39180-6199

and

G. W. Clough

Virginia Polytechnic Institute and State University  
Blacksburg, Virginia 24061



May 1992

Final Report

Approved For Public Release; Distribution Is Unlimited



Prepared for DEPARTMENT OF THE ARMY  
US Army Corps of Engineers  
Washington, DC 20314-1000

# REPORT DOCUMENTATION PAGE

Form Approved  
OMB No. 0704-0188

Public reporting burden for this collection of information is estimated to average 1 hour per response, including the time for reviewing instructions, searching existing data sources, gathering and maintaining the data needed, and completing and reviewing the collection of information. Send comments regarding this burden estimate or any other aspect of this collection of information, including suggestions for reducing this burden, to Washington Headquarters Services, Directorate for Information Operations and Reports, 1215 Jefferson Davis Highway, Suite 1204, Arlington, VA 22202-4302, and to the Office of Management and Budget, Paperwork Reduction Project (0704-0188), Washington, DC 20503.

1. AGENCY USE ONLY (Leave blank)	2. REPORT DATE May 1992	3. REPORT TYPE AND DATES COVERED Final report	
4. TITLE AND SUBTITLE  User's Guide for the Incremental Construction Soil-Structure Interaction Program SOILSTRUCT		5. FUNDING NUMBERS	
6. AUTHOR(S)  R. M. Ebeling, J. F. Peters, G. W. Clough		8. PERFORMING ORGANIZATION REPORT NUMBER  Technical Report ITL-90-6	
7. PERFORMING ORGANIZATION NAME(S) AND ADDRESS(ES)  USAEWES, Information Technology and Geotechnical Laboratories 3909 Halls Ferry Road, Vicksburg, MS 39180-6199 Virginia Polytechnic Institute and State University Blacksburg, VA 24061		9. SPONSORING / MONITORING AGENCY NAME(S) AND ADDRESS(ES)  US Army Corps of Engineers, Washington, DC 20314-1000	
11. SUPPLEMENTARY NOTES  Available from National Technical Information Service, 5285 Port Royal Road, Springfield, VA 22161			
12a. DISTRIBUTION / AVAILABILITY STATEMENT  Approved for public release; distribution is unlimited		12b. DISTRIBUTION CODE	
13. ABSTRACT (Maximum 200 words)  <p>This user's guide is for SOILSTRUCT, a two-dimensional, plane strain finite element program used in the incremental construction, soil-to-structure interaction analysis of earth retaining structures. The initial version of the program was developed by Professors G. W. Clough and J. M. Duncan (1969) for use in the analysis of Port Allen and Old River U-frame locks. The program has been enhanced during the last 20 years by Professor Clough and his coworkers. This version of SOILSTRUCT is available for use on the CRAY Y-MP at the US Army Engineer Waterways Experiment Station (WES) and reflects modifications made in conjunction with a number of projects at WES. These projects include the soil-to-structure interaction analysis of U-frame locks, gravity locks, retaining walls, basement walls, sheet-pile walls, cofferdams, and supported excavations using braced or tieback walls.</p> <p>The finite element method of analysis results in the computation of stresses and displacements for both the structure and the soil backfill. Applications of the procedure to a variety of earth retaining structures have shown the importance of modeling the actual construction process as closely as possible and the use of a nonlinear stress-strain soil model. SOILSTRUCT has the capabilities to simulate incremental construction</p> <p style="text-align: right;">(Continued)</p>			
14. SUBJECT TERMS  Computer programs Finite elements		SOILSTRUCT Soil-structure interaction	15. NUMBER OF PAGES 85
17. SECURITY CLASSIFICATION OF REPORT UNCLASSIFIED		18. SECURITY CLASSIFICATION OF THIS PAGE UNCLASSIFIED	16. PRICE CODE
19. SECURITY CLASSIFICATION OF ABSTRACT		20. LIMITATION OF ABSTRACT	

13. (Concluded).

which may include embankment construction or backfilling, the placement of layer(s) of a reinforcement material during backfilling or embankment construction, dewatering, excavation, installation of a strut or tie-back anchor support system, removal of the same system, and the placement of concrete or other construction materials. In addition, SOILSTRUCT has the capability to include the modeling of the interface region between the soil backfill and the structure, using interface elements.

## PREFACE

This report describes the finite element computer program SOILSTRUCT, used in the evaluation of soil-to-structure interaction of earth retaining structures. The initial version of the program was developed by Professors G. W. Clough and J. M. Duncan in 1969 and has been enhanced during the last 20 years by Professor Clough and his co-workers. This report documents the version of the program that reflects the modifications made in conjunction with project work performed at the US Army Engineer Waterways Experiment Station (WES). This work has been funded by the Numerical Model Maintenance Program.

This report was prepared by Dr. Robert Ebeling, Scientific and Engineering Applications Center, Computer-Aided Engineering Division (CAED), Information Technology Laboratory (ITL), WES, Dr. John F. Peters, Soil and Rock Mechanics Division (SRMD), Soils Research Center (SRC), and Dr. G. W. Clough, Dean of the College of Engineering, Virginia Polytechnic Institute and State University, Blacksburg, VA. The work was managed and coordinated by Dr. Reed L. Mosher, Interdisciplinary Research Group, CAED, ITL. All work was accomplished under the general supervision of Mr. Paul Senter, Chief, CAED, and Dr. N. Radhakrishnan, Chief, ITL. This miscellaneous paper was published by ITL, WES.

At the time of publication of this report, Director of WES was Dr. Robert W. Whalin. Commander and Deputy Director was COL Leonard G. Hassell, EN.

# CONTENTS

	<u>Page</u>
PREFACE . . . . .	1
CONVERSION FACTORS, NON-SI TO SI (METRIC)	
UNITS OF MEASUREMENT . . . . .	3
PART I: DESCRIPTION OF PROGRAM SOILSTRUCT . . . . .	4
Introduction . . . . .	4
Finite Elements Employed . . . . .	4
PART II: MATERIAL STRESS-STRAIN BEHAVIOR . . . . .	6
Nonlinear Stress-Strain Response of Soil . . . . .	6
Primary Loading - Young's Moduli . . . . .	8
Unload-Reload Stress-Strain Behavior - Young's Modulus . . . . .	11
Poisson's Ratio or Bulk Modulus . . . . .	11
PART III: MODELING STRUCTURAL ELEMENTS . . . . .	16
Structural Material Response . . . . .	16
Soil Reinforcement . . . . .	16
Interface Response . . . . .	17
Sheet-Pile Element . . . . .	21
Sheet-Pile Section Properties . . . . .	22
Moment Computations for Bending Members . . . . .	23
Accuracy of Computed Moments . . . . .	24
Elements for Modeling Sheet Pile Cells . . . . .	25
PART IV: USE OF SOILSTRUCT PROGRAM . . . . .	33
Sign Convention And Coordinate System . . . . .	33
Units . . . . .	33
Capacity . . . . .	33
REFERENCES . . . . .	35
APPENDIX A: USER'S GUIDE FOR PROGRAM SOILSTRUCT . . . . .	A1
APPENDIX B: SEQUENCE OF OPERATIONS . . . . .	B1
APPENDIX C: BENDING OF STRUCTURAL MEMBERS . . . . .	C1
APPENDIX D: NOTATION . . . . .	D1

**CONVERSION FACTORS, NON-SI TO SI (METRIC)  
UNITS OF MEASUREMENT**

Non-SI units of measurement used in this report can be converted to SI (metric) units as follows:

<u>Multiply</u>	<u>By</u>	<u>To Obtain</u>
cubic feet	0.2831685	cubic metres
feet	0.3048	metres
pounds (mass) per cubic foot	16.01846	kilograms per cubic metre
pounds (force) per square foot	47.88026	pascals
pounds (force) per square inch	6.894757	kilopascals
square feet	0.09290304	square metres
square inches	6.4516	square centimetres

# USER'S GUIDE FOR THE INCREMENTAL CONSTRUCTION SOIL-STRUCTURE INTERACTION PROGRAM SOILSTRUCT

## PART I: DESCRIPTION OF PROGRAM SOILSTRUCT

### Introduction

1. SOILSTRUCT is a general-purpose, finite element program for two-dimensional, plane strain analysis of soil-structure interaction and soil-inclusion interaction problems. It calculates displacements and stresses due to incremental construction and/or load application and is capable of modeling nonlinear stress-strain material behavior. The simulation of incremental construction may include embankment construction or backfilling, the placement of layer(s) of a reinforcement material during backfilling or embankment construction, dewatering, excavation, installation of a strut or tie-back anchor excavation support system, removal of the same system, and the placement of concrete or other construction materials. The incremental loading simulation may consist of the application of concentrated loads, boundary pressures, or loads due to temperature changes in non-soil materials.

2. The initial version of SOILSTRUCT was developed by Professors G. W. Clough and J. M. Duncan for use in the analysis of Port Allen and Old River U-frame locks (Clough and Duncan 1969). This version of the program reflects modifications made in conjunction with a number of projects at the US Army Engineer Waterways Experiment Station to expand the capabilities of the finite elements constitutive models, load vector formulation algorithms, the size of the problem which may be analyzed, and the transfer of input, output, restart, and plot data files by means of disc storage. SOILSTRUCT has been coded in Fortran 77 language and consists of a main program and 26 subroutines named: DETNA, INITAL, STRSTF, QUAD, BAREL, EXCAV, EQNDFO, SURFLD, JTSTF, SUBSTP, JSTRES, SEEP, MODCAL, BUILD, OPTSOL, AUXOUT, STRESS, PRNCIP, PRNTFD, GETFIL, CNVERT, REBAR, FILLBARS, BARSTIF, RESTRESS, and NFACTS. A user's guide for the SOILSTRUCT Program can be found in Appendix A. Appendix B contains the sequence of operations for the SOILSTRUCT Program. Appendix C applies simple beam theory and the theory of elasticity to the bending of structural members.

### Finite Elements Employed

3. Three types of finite elements are used to represent the behavior of different materials: (a) a two-dimensional continua element, (b) an interface element, and (c) a one-dimensional bar element.

4. A two-dimensional, subparametric, quadrilateral element (QM5) is used to represent the soil and most structural materials. Structural supports, such as the struts or tieback components of an excavation support system, are typically modeled as a spring support using bar elements. However, two-dimensional elements have been used to

model these supports. The geometry of this element, developed by Doherty, Wilson, and Taylor (1969), is defined by four external nodes, while the displacement functions include an internal fifth node. To improve flexural response, a constant shear strain, calculated at the location of the internal fifth node, is imposed throughout the element. The QM5 element can be allowed to degrade to a triangular element by letting two adjacent nodes of the quadrilateral coincide.

5. The Goodman, Taylor, and Breeke (1968) interface element is used to allow for relative movement between different materials, such as between a soil backfill and a support wall. This element is defined by four nodes, with each of the two pairs of nodes having the same coordinates; thus, this type of element has no thickness.

6. One-dimensional, two-node, bar or spring elements are used to model the behavior of a variety of structural systems. This includes the modeling of structural supports such as braces or tiebacks or the modeling of reinforcement placed within a soil backfill.

## PART II: MATERIAL STRESS-STRAIN BEHAVIOR

7. Several modes of stress-strain behavior are utilized to represent the response of soil, construction materials, and the interface region between different materials.

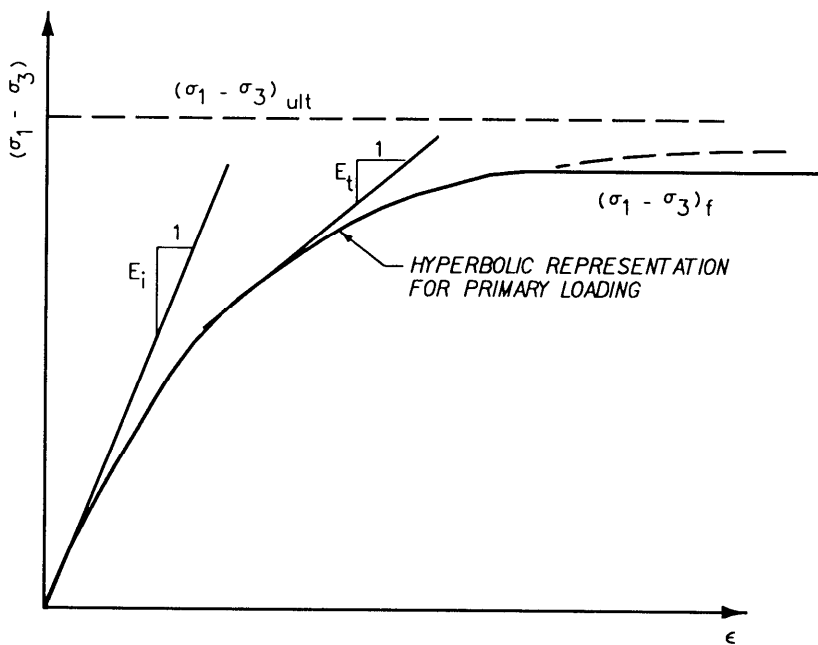
8. The constitutive relationship used for all two-dimensional elements is Hooke's law. SOILSTRUCT uses an incremental, equivalent linear method of analysis to model nonlinear material behavior. In this type of analysis, the incremental changes in stresses are related to the incremental strains through a linear relationship. This relationship is defined for each structural element by two engineering constants, the Young's moduli and the Poisson's ratio. For the soil elements, either the Young's moduli and Poisson's ratio, or the Young's moduli and bulk moduli may be specified.

### Nonlinear Stress-Strain Response of Soil

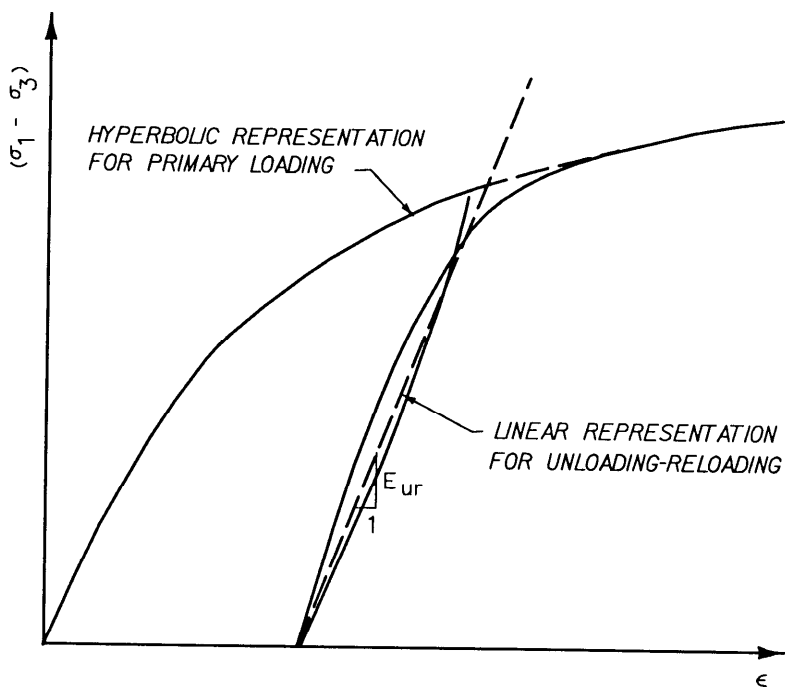
9. A plane strain, isotropic drained or undrained stress-strain soil model is incorporated within SOILSTRUCT. The program uses a nonlinear, stress-dependent hyperbolic curve to represent the relationship between stress and strains developing during primary loading of the soil (Figure 1a) and a linear stress-strain response during unloading or reloading of the soil (Figure 1b). The unload-reload stress-strain response is applicable when the current stress state is less than that which has been applied previously; otherwise, the primary loading stress-strain is appropriate. Laboratory testing and interpretation procedures for determining the parameters used to define the soil model are described in Duncan, Byrne, Wong, and Mabry (1978). A brief review of the hyperbolic model is given in paragraphs 12-17.

10. The nonlinear soil response to loading is modeled by performing a series of analyses in which each load is applied incrementally, with the total change in stress computed at the center of each soil element being equal to the sum of the incremental changes in stress over all the load steps. In general, the greater the curvature of the stress-strain relationship or the larger the magnitude of the applied load, the greater the number of load steps required to accurately model the nonlinear soil response. This may be achieved in two ways using SOILSTRUCT; either the total load is applied using a greater number of incremental loadings, or during the course of each load case analysis, the load vector may be applied in a series of increments using the sub-step option.

11. Application of each loading in the finite element analysis results in a change in stress within each of the soil elements. In addition to the change in stress, there is a corresponding change in stiffness. Since each incremental analysis is performed assuming equivalent linear element response, SOILSTRUCT updates the value of the elastic moduli assigned to each soil element so as to reflect the magnitude of the current stress state within the element. To account for the change in stiffness that occurs during the application of a load increment, each incremental load calculation may be repeated using the iteration option. When the iteration option is invoked, the load vector is reapplied with a revised value for the element stiffness. The value assigned for the stiffness



a. Hyperbolic representation of stress-strain curve for primary loading



b. Linear unloading-reloading stress-strain relationship

Figure 1. Hyperbolic model for stress-strain behavior (after Duncan, Byrne, Wong, and Mabry 1978)

of the soil element reflects the average of the stress state developing at the end of the previous load case, or substep, and that which develops during the current iteration. However, when only one iteration is specified, the modulus values are calculated using the stresses developing at the end of the previous load increment. Upon completion of the last iteration for each load case or substep, the arrays tabulating the values of the total nodal point displacements and total element stresses are updated with the computed incremental values.

### Primary Loading - Young's Moduli

12. Prior to each analysis a tangent Young's modulus  $E_t^*$  is assigned to each soil element. The stress-dependent value of  $E_t$  is computed using the relationship

$$E_t = E_i \left( 1 - R_f \cdot SL \right)^2 \quad (1)$$

where

$E_i$  = initial Young's modulus

$R_f$  = failure ratio

$SL$  = stress level

The initial Young's modulus  $E_i$  is equal to

$$E_i = K P_a \left( \frac{\sigma_3}{P_a} \right)^n \quad (2)$$

where

$K$  = modulus number

$P_a$  = atmospheric pressure

$n$  = modulus exponent

$\sigma_3$  = minor principal stress

13. The proportion of mobilized shear strength for each soil element is reflected in the value of the stress level,  $SL$ .  $SL$  is equal to the current deviator stress  $(\sigma_1 - \sigma_3)$  divided by the deviator stress at failure  $(\sigma_1 - \sigma_3)_f$ , denoted by the subscript  $f$ .

---

\* For convenience, symbols and abbreviations are listed in the Notation (Appendix D).

$$SL = \frac{\sigma_1 - \sigma_3}{(\sigma_1 - \sigma_3)_f} \quad (3)$$

where  $\sigma_1$  = major principal stress. The value of SL ranges from a value equal to zero to a value equal to unity. SL equal to zero indicates an isotropic stress state, while SL equal to unity corresponds to the complete mobilization of shear resistance within the soil element.

14. This version of SOILSTRUCT allows for two procedures for defining the deviator stress at failure; the original Duncan formulation, Duncan and Chang (1970), and a procedure developed by Peters. In the original Duncan formulation as shown in Figure 2a, the value of the minor principal stress at failure is set equal to the current minor principal stress. The deviator stress at failure is given by

$$(\sigma_1 - \sigma_3)_f = \frac{2c \cos \phi + 2\sigma_3 \sin \phi}{1 - \sin \phi} \quad (4)$$

where

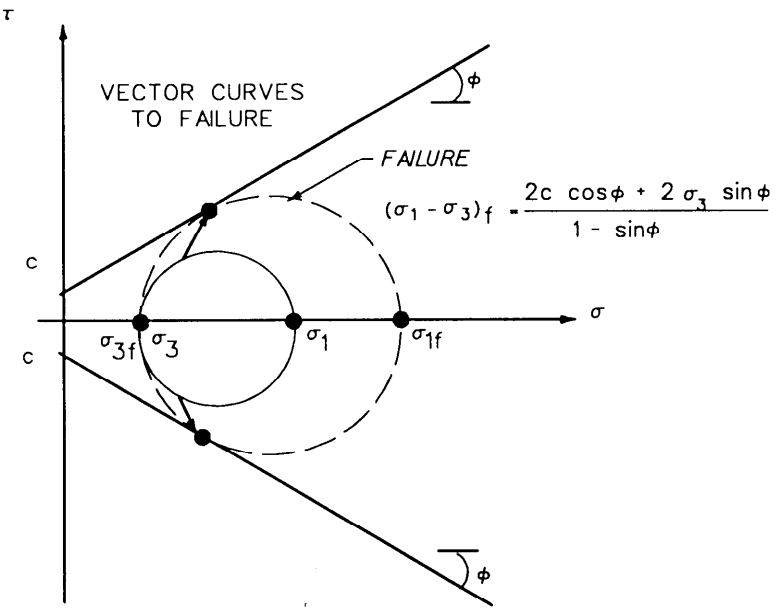
$c$  = cohesion intercept

$\phi$  = angle of internal friction

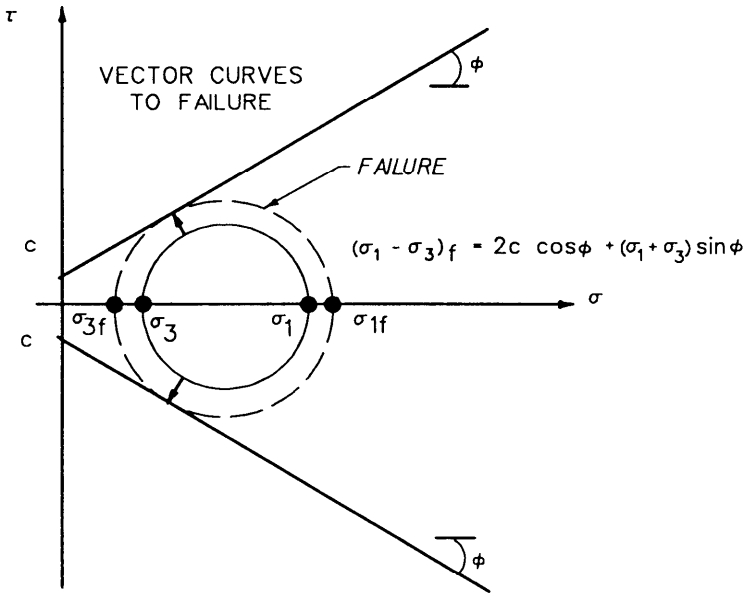
In the Peters formulation shown in Figure 2b, the value for the deviator stress at failure is defined based upon the assumption that the average value of the major and minor principal stresses at failure is equal to the average value of the current major and minor principal stresses.

$$(\sigma_1 - \sigma_3)_f = 2c \cos \phi + (\sigma_1 + \sigma_3) \sin \phi \quad (5)$$

15. The difference between these two procedures may be expressed in terms of the resulting vector curves as shown in Figure 2. Vector curves are loci of points describing the state of stress on planes on which failure eventually occurs. The resulting vector curves in the Duncan formulation are to the right, reflecting the assumption that failure is a result of an increase in major principal stress. In contrast, the vector curves to the left in the Peters formulation are attributed to a coincident increase in major principal stress and a decrease in the minor principal stress. In general, the Duncan formulation results in larger values of  $(\sigma_1 - \sigma_3)_f$  and therefore smaller values of SL than the Peters formulation. The Peters formulation was developed for undrained loading where  $(\sigma'_1 + \sigma'_3)$  is the **constant** consolidation stress determined for the initial stress state.



a. Duncan formulation,  $\sigma_{3f} = \sigma_3$



b. Peters formulation,  $p = \frac{(\sigma_1 + \sigma_3)_f}{2} = \frac{(\sigma_1 + \sigma_3)}{2}$

Figure 2. Two procedures used to define deviator stress at failure,  $(\sigma_1 - \sigma_3)_f$

16. The failure ratio  $R_f$  relates the ultimate deviator stress  $(\sigma_1 - \sigma_3)_{ult}$  to the deviator stress at failure  $(\sigma_1 - \sigma_3)_f$ .

$$(\sigma_1 - \sigma_3)_f = R_f (\sigma_1 - \sigma_3)_{ult} \quad (6)$$

The ultimate deviator stress is the asymptote to the stress-strain hyperbola, as shown in Figure 1a. The value of  $R_f$  is always less than unity and varies from 0.5 to 0.9 for most soils.

### Unload-Reload Stress-Strain Behavior - Young's Modulus

17. During unloading or reloading, when the current deviator stress is less than that which has been applied during previous loadings, a stress-dependent, linear response is assumed, as shown in Figure 1b. In this case, the value of  $E_{ur}$  is computed using

$$E_{ur} = K_{ur} P_a \left( \frac{\sigma_3}{P_a} \right)^n \quad (7)$$

where  $K_{ur}$  = the unload-reload modulus number.

### Poisson's Ratio or Bulk Modulus

18. The second elastic parameter used to define the material behavior of soil is either the Poisson's ratio,  $\nu$ , or the bulk modulus,  $B$ . This version of SOILSTRUCT allows either parameter to be used. When using Poisson's ratio, two values are specified: a constant value which is applicable for all states of stress prior to failure,  $SL < 1$ , and the value of Poisson's ratio applicable when the shear strength of the soil is fully mobilized,  $SL = 1$ .

#### Poisson's ratio formulation

19. The hyperbolic model is designed so that as the soil approaches failure,  $\nu = 0.5$ . The variation in  $\nu$  is accomplished by computing the shear modulus with  $E_t$  and  $\nu_i$  and bulk modulus with  $E_i$  and  $\nu_i$ , where  $\nu_i$  is the value of Poisson's ratio before failure. This variation in  $\nu$  amounts to

$$\nu = \frac{1}{2} \left( \frac{1 - b}{1 + \frac{1}{2}b} \right) \quad (8)$$

where

$$b = \left( \frac{E_t}{E_i} \right) \left( \frac{1 - 2\nu_i}{1 + \nu_i} \right) \quad (9)$$

Therefore,  $\nu = \nu_i$  when  $E_t = E_i$ , but increases toward 0.5 as  $E_t$  becomes small near failure.

### Bulk modulus formulation

20. Because many soils exhibit nonlinear and stress-dependent volume change characteristics, the stress-dependent bulk modulus formulation developed by Duncan, Byrne, Wong, and Mabry (1978) is also included. According to the theory of elasticity the value of the bulk modulus  $B$  is defined as the ratio of the change in mean principal stress to the change in the volumetric strain.

$$B = \frac{\Delta\sigma_1 + \Delta\sigma_2 + \Delta\sigma_3}{3\varepsilon_v} \quad (10)$$

where  $\Delta\sigma_1$ ,  $\Delta\sigma_2$ , and  $\Delta\sigma_3$  are the changes in the values of principal stress and  $\varepsilon_v$  is the corresponding change in volumetric strain.

21. The bulk modulus for soil has been found to increase in value with increasing values of minor principal stress and is assumed to be independent of stress level. It is approximated by the equation

$$B = K_b P_a \left( \frac{\sigma_3}{P_a} \right)^m \quad (11)$$

where

$K_b$  = bulk modulus number

$m$  = bulk modulus exponent

22. Experience with this formulation, as described by Duncan, Seed, Wong, and Ozawa (1984), has led to the following restrictions on the value assigned to the bulk moduli. The maximum value of bulk moduli corresponds to the situation when the value for Poisson's ratio  $\nu$  is equal to 0.49. The value of bulk moduli may be defined by the values of Young's modulus  $E_t$  and  $\nu$  as given by the relationship

$$B = \frac{E_t}{3} \left[ \frac{1}{(1 - 2\nu)} \right]$$

The bulk moduli attains a maximum value when  $\nu = 0.49$  and is equal to

$$B_{\max} = 17 (E_t) \quad (13)$$

23. The value assigned for the bulk modulus is also restricted to a minimum value. This minimum value is determined from the relationships between bulk modulus, Poisson's ratio, the at-rest earth pressure coefficient  $K_o$ , and the angle of internal friction  $\phi$ . For a single linear elastic material (Dunlop, Duncan, and Seed 1968)  $K_o$  and  $\nu$  are related as follows:

$$\nu = \frac{K_o}{1 + K_o} \quad (14)$$

Jaky (1948) suggested that  $K_o$  may be approximated using the relationship

$$K_o = 1 - \sin \phi \quad (15)$$

By introducing Equations 14 and 15 into Equation 12, the minimum value for the bulk moduli value during primary loading is restricted to

$$B_{\min} = \frac{E_t}{3} \left[ \frac{(2 - \sin \phi)}{\sin \phi} \right] \quad (16)$$

Experience gained when using this soil model to simulate excavation resulted in the development of the restriction on the value of bulk moduli during unloading-reloading behavior as given by

$$B_{\min} = \frac{E_t}{3} \frac{(1 + K_o)}{(1 - K_o)} \quad (17)$$

This relationship was obtained by introducing Equation 14 into Equation 12.

### **Consolidation stress method for undrained analysis**

24. Soil strength is typically defined in SOILSTRUCT by cohesion  $c$  and friction angle  $\phi$ , which are chosen to be appropriate for the drainage condition of each element based on its permeability and the loading rate. For undrained conditions, how-

ever, this approach is not suitable. In order to model the increase in strength produced by higher consolidation stress it is necessary to either assign a different cohesion (with  $\phi = 0$ ) to each element, which is not practical, or to assign a total stress friction angle to each material, which is physically inconsistent for saturated materials. The correct result can only be obtained for undrained conditions by selecting the undrained strength from the preloading consolidation conditions and setting  $\phi = 0$  for all subsequent undrained loadings. Therefore, the program allows the strength to be input as a ratio of strength to effective consolidation pressure ( $S_u/p'_c$ ). Likewise,  $n$  is set to zero and  $K$  is expressed as a function of the initial consolidation stress; this is an approach similar to that described below for soil strength whereby the strength is based on the initial consolidation state and the friction angle is set to zero. It has been found through experience that the initial modulus,  $P_a K$ , can be expressed as a ratio of the undrained shear strength (Clough and Tsui 1977; Mana 1978) whereby  $E_i = \bar{K} S_u$ . Thus, assuming the constant  $\bar{K}$  is known, the undrained shear strength becomes the fundamental parameter controlling the response of the soil. The procedure consists of the following:

- a. The consolidation stress is computed for each element based on the geometry and boundary conditions prior to loading assuming that the pre-existing elements have fully consolidated under their own weight. Elements above the water table are assigned the total unit weight of the soil, and elements below the water table are assigned the buoyant unit weight. The stresses created by this configuration are computed by subroutine INITAL.
- b. The effective consolidation stress  $p'_c$  is computed for each element as

$$p'_c = \frac{1}{2} (\sigma'_h + \sigma'_v) \quad (18)$$

where  $\sigma'_h$  and  $\sigma'_v$  are, respectively, the horizontal and vertical effective stresses. This value is stored for each element for use in all subsequent calculations.

- c. Each material type is assigned a value of  $S_u/p'_c$  and  $\bar{K}$ . These values are then combined with  $p'_c$  computed from the initial stress computations to determine  $S_u$  and  $E_i$  for each element. The property values assigned to each element therefore depend on material type and section geometry. For example, shear strengths may be moderately higher under a levee centerline than at the toe as a result of the higher consolidation stress imposed by the levee.

### Poisson's ratio for initial stress computation

25. When computing initial stresses by gravity turn-on analysis, the value of Poisson's ratio used for the soil model may not be suitable for initial stress conditions.

For example, the Poisson's ratio for undrained analysis is generally taken to be nearly 0.5 because saturated soil is nearly incompressible. By contrast, the initial stress conditions should be fully drained. Therefore, the initial stress computations are based on a value of Poisson's ratio that gives the correct ratio  $\sigma'_v / \sigma'_h$  for level ground conditions; that is,  $\sigma'_v / \sigma'_h = K_o$ . Using the value of  $K_o$  input, the Poisson's ratio used for initial conditions is given by Equation 14.

## PART III: MODELING STRUCTURAL ELEMENTS

### Structural Material Response

26. Structural materials such as wood, concrete, or steel are modeled using two-dimensional QM5 elements with linear elastic stress-strain behavior assumed. Support elements such as struts or anchors are typically modeled using one-dimensional bar elements, and are also assumed to behave linearly. Bar elements as formulated within SOILSTRUCT have the capability to respond in compression only, in tension only, or in both tension and compression. In addition, slack in the support system at the time of installation may be accounted for by specifying an initial value of displacement for the bar element.

### Soil Reinforcement

27. Reinforcement placed within a soil backfill provides resistance to tensile strains which may develop as a result of loadings attributed to the force due to gravity acting on the soil mass or due to applied loadings. The reinforcement within a soil backfill or an embankment is modeled using one-dimensional bar elements. Reinforcement has the effect of increasing the stiffness of the soil mass and is modeled by increasing the stiffnesses of each of the two-dimensional soil elements that includes a layer of reinforcement.

28. Reinforcement can be modeled by either of two methods. The first method consists of using bar elements, as tension-only elements, sandwiched between solid elements. By this method the location of reinforcing must be accounted for in laying out the analysis mesh. This may become inconvenient if reinforcing layers are closely spaced.

29. The second method allows the reinforcing to be “embedded” into the interior of the element such that it is unnecessary to place reinforcement at element boundaries. The stiffness of the reinforcement is added to the solid element as follows: the stiffness for the reinforcement “bar” element,  $[K_b]$ , which defines the relationship between the displacement  $\{u_b\}$  and the bar forces, is then related to the node displacements  $\{u\}$  by the interpolation  $\{u_b\} = [N]\{u\}$ , where  $[N]$  is the interpolation matrix for displacement. Thus the effect of the bar on the element stiffness is obtained by adding to it the quantity  $[N]^T[K_b][N]$ . The procedure can be repeated for any number of bars placed at any orientation within the element. Also, the procedure does not add to the total number of degrees of freedom. The only input required to add reinforcement by method two is the stiffness and location of the reinforcement **layer**; the individual soil elements affected by the layer are determined by SOILSTRUCT.

30. During each analysis the reinforcement model monitors the resulting total strains within each bar element and distinguishes between tensile and compressive strains. Typical soil reinforcement materials are very thin relative to their length and are not capable of resisting compressive strains. This restriction is incorporated within the reinforcement model by reducing the reinforcement bar stiffness to a near zero value when

compressive strains are computed. The model has a provision for re-establishing the tensile stiffness of the reinforcement bar element(s) to the two-dimensional soil element(s) when and if tensile strains occur within the bar(s) during subsequent loadings.

### Interface Response

31. Interface elements are used to allow for relative movement between different material regions, such as between a soil backfill and a support wall. These elements are defined by four nodes, each node having two degrees of freedom; each of the two pairs of nodes sharing the same coordinates. The interface element, therefore, is of finite length but zero thickness.

32. The properties of interface elements are defined by an interface normal stiffness  $k_n$  and an interface shear stiffness,  $k_s$ . These values of stiffness relate the average relative displacements normal to the interface element  $\Delta_n$  and average relative shear displacements  $\Delta_s$  to the corresponding normal stress  $\sigma_n$  and shear stress  $\tau$  by the equations

$$\sigma_n = k_n \Delta_n \quad (19)$$

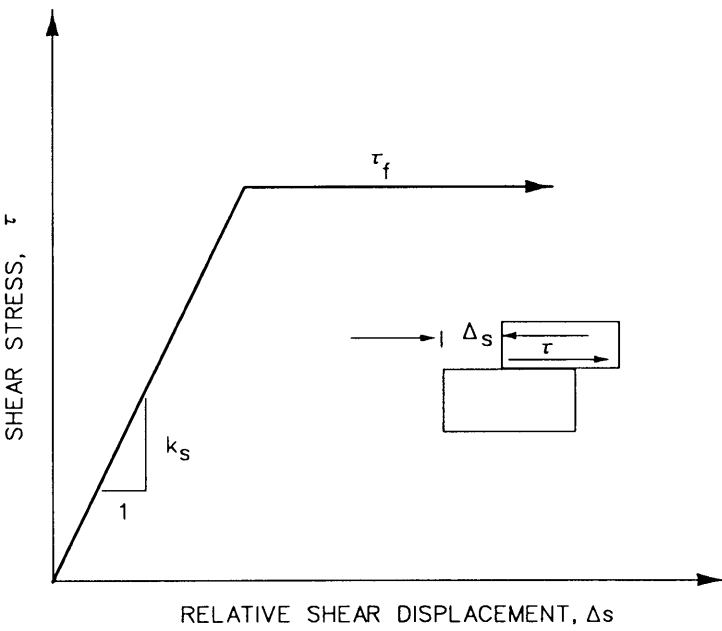
and

$$\tau = k_s \Delta_s \quad (20)$$

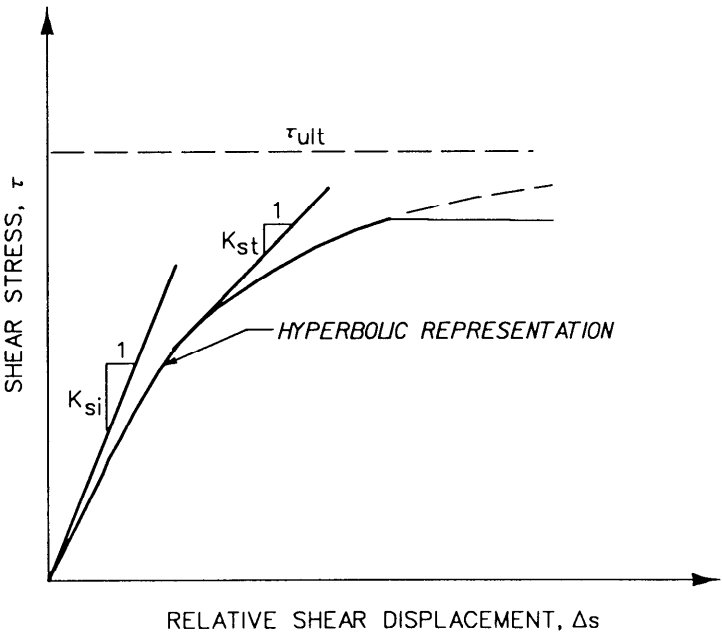
The units of  $k_n$  and  $k_s$  are force per cubic length.

33. The initial value of  $k_n$  is set equal to  $1 \times 10^8$  within the program. This value for  $k_n$  ensures that the normal relative displacement of the interface element is insignificant when English units (feet, pounds) or SI units (meters, kilonewtons) are used. If other units are used, the value of the normal stiffness may need to be changed to a higher value.

34. Two types of interface shear response are modeled, a bilinear shear stress-displacement relationship shown in Figure 3a, and a hyperbolic shear stress-displacement relationship shown in Figure 3b. In the bilinear model, the value assigned to  $k_s$  is a constant so long as the average shear stress  $\tau$  along the interface is less than the shear strength. If the shear strength of the interface element is fully mobilized, which occurs when  $\tau$  is equal to  $\tau_f$ ,  $k_s$  is set equal to zero. When the normal stress  $\sigma_n$  is greater than or equal to zero, the value of  $\tau_f$  is given by the relationship



a. Bilinear stress-strain model representing interface behavior



b. Hyperbolic representation of the variation of shear stress with relative shear displacement ( $k_{st}$  = tangent interface shear stiffness,  $k_{si}$  = initial interface shear stiffness)

Figure 3. Bilinear and hyperbolic models for interface shear stress-relative shear displacement behavior after Clough and Duncan (1969)

$$\tau_f = c_i + \sigma_n \tan \delta \quad (21)$$

where

$c_i$  = cohesion intercept along the interface

$\delta$  = angle of internal friction along the interface

and shown in Figure 4a. When  $\sigma_n$  is less than zero,  $\tau_f$  is computed using

$$\tau_f = \sigma_n \left( \frac{c_i}{\sigma_t} \right) \quad (22)$$

where  $\sigma_t$  = tensile strength.

35. Direct shear test results on soil-to-concrete interfaces and soil-to-steel interfaces by Potyondy (1961), Clough and Duncan (1969), and Peterson et al. (1976) have shown that the value of  $\delta$  is proportional to the angle of internal friction of the soil. The value of the constant of proportionality is dependent upon both the type of soil and the type of material comprising the surface of the structure.

36. The direct shear tests performed by Clough and Duncan (1969) and Peterson et al. (1976) have shown that for some materials, such as sand-to-concrete interfaces, the interface response during shear is nonlinear and dependent upon the normal stress. A nonlinear, stress-dependent hyperbolic curve is used to represent the relationship between shear stress and average relative shear displacement developing during primary loading of the interface (Figure 3a) and a linear shear stress-relative displacement response during unloading or reloading of the interface. The stress-dependent value of  $k_{st}$  is computed using the relationship

$$k_{st} = k_{si} (1 - R_{fi} \cdot SL_i)^2 \quad (23)$$

where

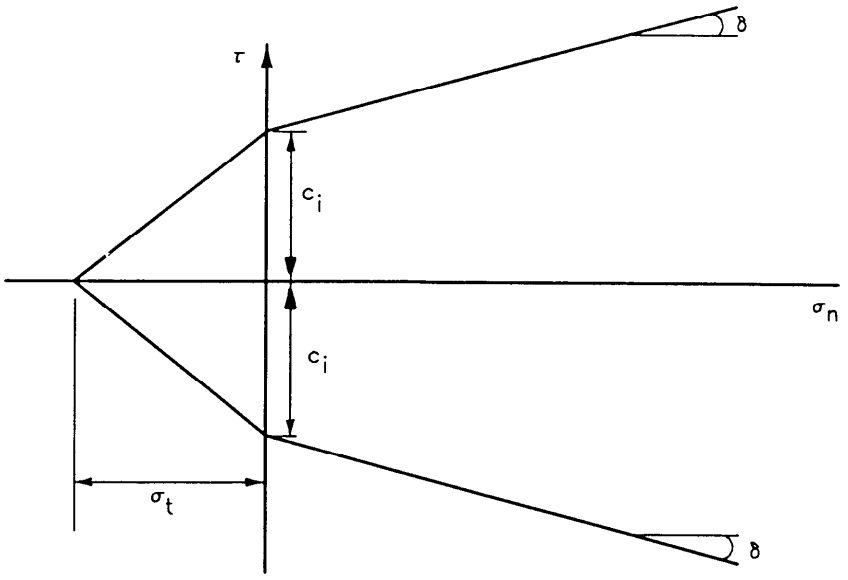
$k_{si}$  = initial interface shear stiffness

$R_{fi}$  = failure ratio

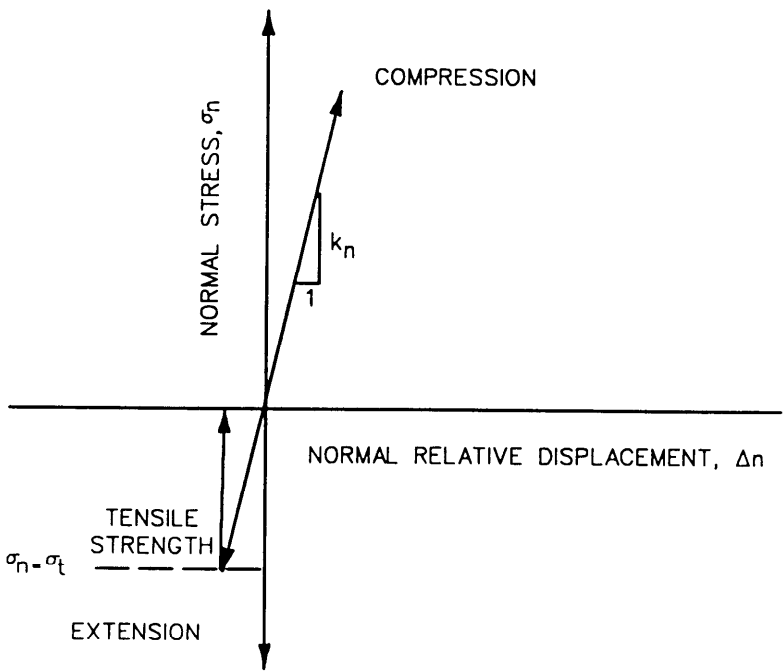
$SL_i$  = stress level

The initial interface shear stiffness  $k_{si}$  is equal to

(24)



a. Strength criteria



b. Normal stress-normal relative displacement behavior

Figure 4. Interface strength criteria and normal stress-normal relative displacement relationship

$$k_{si} = K_j \gamma_w \left( \frac{\sigma_n}{P_a} \right)^{n_i}$$

where

$K_j$  = interface modulus number

$\gamma_w$  = unit weight of water

$n_i$  = interface modulus exponent

37. The proportion of mobilized shear strength for each interface element is reflected in the value of the stress level  $SL_i$ .  $SL_i$  is equal to the current shear stress  $\tau$  divided by the stress at failure,  $\tau_f$ .

$$SL_i = \frac{\tau}{\tau_f} \quad (25)$$

$\tau_f$  is computed using either Equation 21 or 22.  $SL_i$  ranges in value between zero and one.

38. The failure ratio  $R_{fi}$  relates the ultimate shear stress  $\tau_{ult}$  to the shear stress at failure.

$$\tau_f = R_{fi} \cdot \tau_{ult} \quad (26)$$

The ultimate shear stress is the asymptote to the shear stress-relative shear displacement hyperbola, as shown in Figure 4b. Direct shear tests on sand-to-concrete interfaces by Peterson et. al (1976) have shown the value of  $R_{fi}$  typically ranges in value from 0.3 to 1.0.

39. The relationship between the average normal stress along the interface and the tensile strength is shown in Figure 4b. The value of  $k_n$  is a constant value equal to  $1 \times 10^8$  when  $\sigma_n$  is greater than or equal to  $\sigma_t$ . If  $\sigma_n$  is less than  $\sigma_t$ ,  $k_n$  is set equal to zero, assuring that additional tensile stresses do not accrue upon subsequent loadings. This procedure allows for separation to occur between two adjacent regions of the mesh along interface elements during the course of an incremental analysis. If the separation closes during subsequent loading,  $k_n$  is reset to  $1 \times 10^8$ .

## Sheet-Pile Element

40. Due to the slenderness of sheet piles, their primary mode of response to earth and water loadings is the development of bending stresses within the sheet pile. Thus, the response of the finite element used to model the sheet pile in bending is of primary importance. Representation of bending stiffness in soil-structure interaction analyses has always presented a difficulty. If an element is formulated for bending using the approach found in most structural analysis codes, an incompatibility is created between the bending and solid (soil) elements. This incompatibility results from the technical requirement that displacement gradients (slope) must be continuous across beam elements whereas the solid elements generally only provide for continuous displacements. The incompatibility problem is avoided in SOILSTRUCT by using slender solid elements to model bending. These elements are similar to the soil elements, rather than true beam elements. In fact, the particular choice of element formulation selected for the SOILSTRUCT code was made to ensure that the solid elements would correctly model strain patterns associated with bending. Experience by Mana (1978) on a number of soil-structure interaction problems has shown this approach to work well.

### Sheet-Pile Section Properties

41. The properties of the solid elements used to model the sheet pile are the elastic properties,  $E$  and  $\nu$ . However, the stiffness of flexural members depends on the product  $EI$  where  $I$  is the moment of inertia, a geometric property of the member's cross section. The finite element has a rectangular cross section having a unit width (in the out-of-plane direction) and a height that depends upon how the analysis mesh is drawn. For example, a sheet-pile wall has a complex cross-sectional shape, but is represented in the finite element mesh as a unit-wide rectangle with a height that depends on such considerations as maintaining an aspect ratio of the finite element that is favorable from a standpoint of numerical accuracy. To achieve the response to bending that is consistent with simple beam theory (see section titled "Simple Beam Theory" in Appendix C), the modulus of the element must be chosen to obtain the equivalent flexural stiffness as specified by the product  $EI$ , where  $I$  is the moment of inertia per unit width of sheet pile wall. Therefore, the properties of the sheet-pile elements are determined such that the section stiffness of the plane strain element  $E_e I_e / (1 - \nu_e^2)$  (see section titled "Pure Bending of Members in Plane Strain" in Appendix C) matches the  $EI$  of the sheet pile. Therefore, the sheet pile elements obtain proper bending stiffness when assigned the modulus given by:

$$E_e = \frac{EI}{I_e} (1 - \nu_e^2) \quad (27)$$

where

$E_e$  = equivalent Young's modulus for pile elements

$E$  = Young's modulus for the sheet pile

$I$  = moment of inertia per unit width of sheet-pile wall

$I_e$  = equivalent moment of inertia of the element used to model the sheet pile

$$I_e = \frac{1}{12} b_e h_e^3 \quad (28)$$

and

$b_e$  = unit width of the sheet-pile wall mesh

$h_e$  = width of the element used to model the sheet pile

$\nu_e$  = Poisson's ratio of the element used to model the sheet pile

The factor  $(1 - \nu_e^2)$  comes about due to plane strain considerations (see section titled "Pure Bending of Moments in Plane Strain" in Appendix C).

### Moment Computations for Bending Members

42. While use of solid elements for bending members works well to represent the stiffness provided by bending, the problem remains as to how to compute moments. The solid element representation naturally provides statically equivalent stress values at the center of the element; these values cannot be related to a bending moment. One

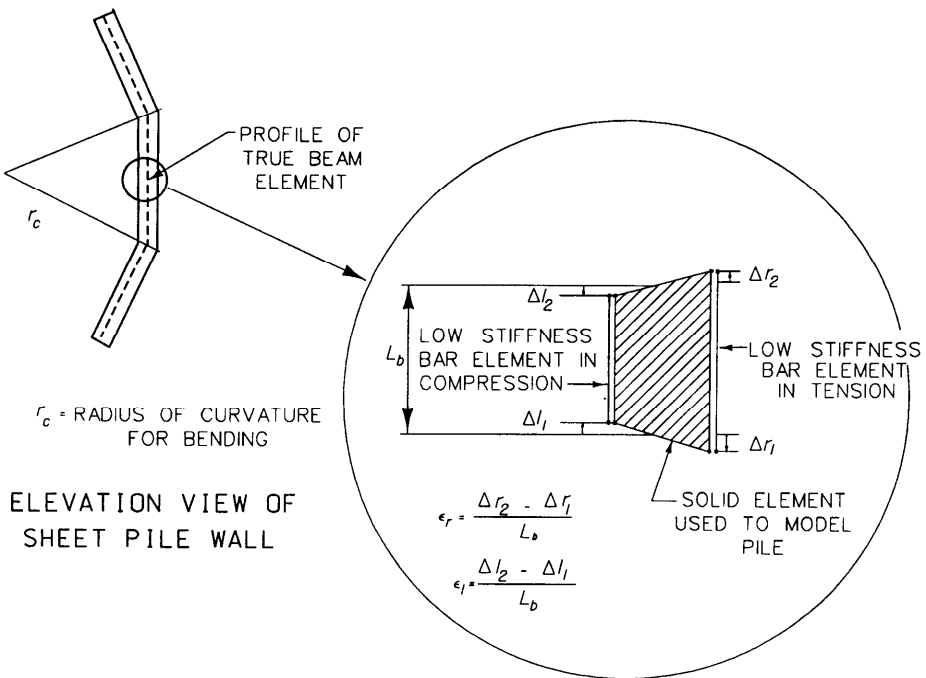


Figure 5. Strain gage method of computing bending moments for four-node solid element (Leavell et al. 1989)

method used for computing moments is based on the premise that moments could be computed from beam theory using the “outer fiber strains” computed from displacements of the end nodes. This process is illustrated in Figure 5, which shows the solid elements in a bending pattern. The outer fiber strains are shown to be related to a radius of curvature that a true beam element would conform to. As an expedient, the outer fiber strains are computed by placing bar elements on the edges of the beam elements. These “strain gage” elements are created by using the standard bar element provided by SOILSTRUCT (for modeling anchors and struts, etc.). The bar was given a low stiffness so that there was virtually no interaction between the bar element and surrounding elements. The strains measured in the two bars are therefore the outer fiber strains  $\epsilon_r$  and  $\epsilon_l$ . These strains may be related to the bending strain  $\epsilon_b$  and axial strain  $\epsilon_a$  as follows:

$$\epsilon_a = \frac{1}{2}(\epsilon_r + \epsilon_l) \quad (29)$$

$$\epsilon_b = \frac{1}{2}(\epsilon_r - \epsilon_l) \quad (30)$$

For the case of pure bending (no axial load)  $\epsilon_r = -\epsilon_l$  and  $\epsilon_a = 0$ . For purely axial loads  $\epsilon_r = \epsilon_l$  and  $\epsilon_b = 0$ . \* Once the strains have been computed the moment per unit width of sheet-pile wall is obtained from the following (see section titled “Pure Bending of Members in Plane Strain” in Appendix C):

$$M = 2 \frac{E_e I_e}{h_e (1 - \nu_e^2)} \epsilon_b \quad (31)$$

The factor of 2 in the above equation results from the depth to neutral axis of one half the width,  $h_e$ , of the corresponding sheet-pile element.

### Accuracy of Computed Moments

43. Leavell et al. (1989) investigated the ability of the strain-gage method to accurately predict moments by comparing the moments computed in a finite element analysis of a fixed end beam with the moments computed using classical beam theory for the same cantilever beam. They found that when the Poisson’s ratio is set equal to 0 in the finite

---

\* Note that a stiffness could be given to the bar to customize the beam element for unsymmetrically reinforced concrete walls, etc., or to model tensile cracking of walls by using a compression-only bar. Also, pure shear deformation of the pile causes no strain in the bars, a fact that could be of some importance since the moment of inertia (I) scales as the cube of the pile thickness whereas the shear stiffness is proportional to thickness. Thus, the bars could be used to add stiffness to bending without changing shear behavior.

element analysis, the computed results differed from those results computed using classical beam theory by 0.01 percent.

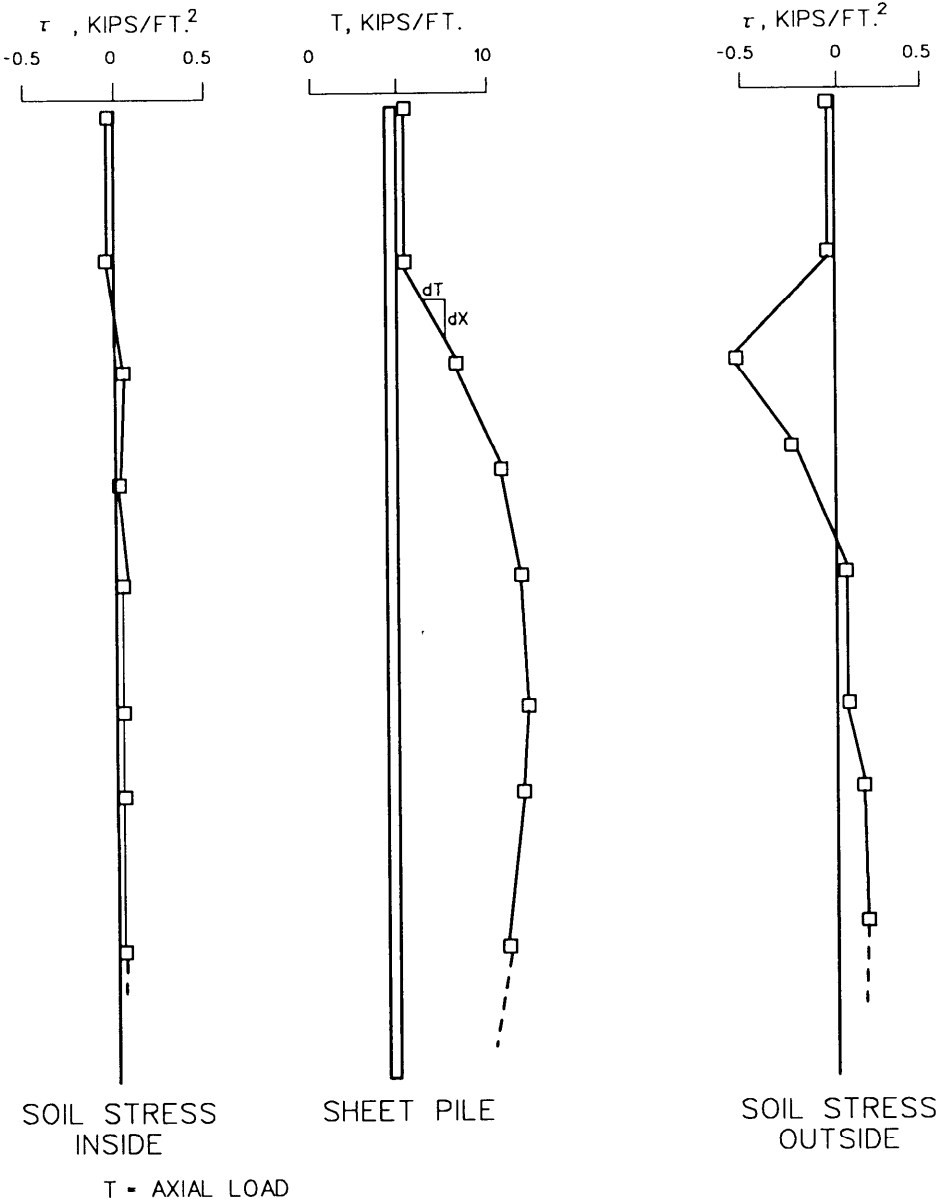
44. The displacement along the beam is approximated by the solid element as a series of straight lines. (If, instead, the beam is represented by a true bending element, the displacement would be represented by a smooth curve.) As a result, the bending moment computed for the element represents an average value that is presumably indicative of the value at the center of the element. Mosher and Knowles (1990) showed that the resolution can be improved by using more elements to represent the pile and by using elements with smaller aspect ratios to model the pile. However, the important feature of the solid elements is that, in contrast to standard beam elements, they deform in a manner that is compatible with adjacent soil elements, a consideration of far greater importance than the small error inherent with the linear approximation.

### **Elements for Modeling Sheet Pile Cells**

45. SOILSTRUCT can be used for analysis of rows of sheet pile cells by considering an "equivalent" planar slice through the row (Clough and Kuppusamy 1985). Determination of properties for the sheet-pile elements is complicated by two aspects of the problem, (a) the arcuate-shaped cells are modeled by a planar slice that represents the average behavior of the main and arc cells and (b) the sheet-pile properties represent an average behavior of the web and interlocks.

46. To address the first problem created by the planar representation, the action of the sheet piles was depicted by Clough and Kuppusamy (1985) as consisting of three independent parts; the outermost (riverward and landward) sheet piles represented as sheet-pile walls using solid elements, the hoop stiffness of the cell represented by horizontal springs connecting the outside walls, and sheet piles separating the main and arc cells represented as shear walls.

47. The justification for the planar representation depends on the independence of the three cell components described above. The independence of the three components, in turn, depends on the small flexural rigidity of the sheet piles that make up the cells. Because very little resistance is derived through bending, the axial stiffness of the sheet piles is the principal structural component of the outside walls. Therefore, the vertical resistance derived from the arcuate-shaped wall can be modeled by a planar wall reasonably well. To illustrate how shear resistance is derived from axial sheet pile stiffness, the equilibrium of the sheet pile-soil system is shown in Figure 6. The ability of the pile to sustain axial loads permits a jump in shear stress across the pile equal to the gradient in axial load along the pile. Without the pile, a continuous horizontal shear-rupture plane could form, causing a sliding failure. With the pile in place, the shearing stress is distributed along the pile, and for the cell to fail, vertical shear failure must occur along the length of the wall. The correspondence between the jump in shear stress across the sheet-pile wall and the gradient of axial pile force from a typical analysis can be seen clearly in Figure 6.



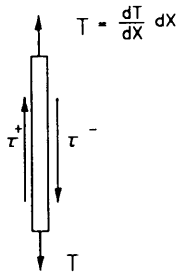
SOIL STRESS  
INSIDE

SHEET PILE

SOIL STRESS  
OUTSIDE

T = AXIAL LOAD

DIFFERENTIAL  
LENGTH  
OF  
SHEET PILE =  $dx$



$$\tau^+ - \tau^- = \frac{dT}{dx}$$

Figure 6. Example of stress transfer from soil to sheet pile  
(Peters, Holmes, and Leavell 1986)

48. The hoop stresses carried by the springs respond primarily to changes in lateral loads and are thus most important during cell filling, excavation, and flood loading. The lateral stress developed in the cell fill and the sheet-pile interlock forces depend directly on the hoop stiffness. The springs closely approximate the hoop stresses, provided the shear stress carried by the sheet piles is small. It has been observed from analysis that the spring stiffness does not directly influence the shear resistance of the cell. The shear resistance of the cell is derived from the outside walls and the shear resistance of the soil. The springs contribute to shear resistance by laterally confining the cell fill.

### Outside wall solid elements

49. The properties of the solid elements making up the outside walls are selected to match the axial stiffness for a unit length of cofferdam. For example, Peters et al. (1986) used a solid sheet-pile element 1 ft depth with a modulus of  $4.6 \times 10^8$  psf, a combination of thickness and modulus that gave an equivalent stiffness of the sheet piling while not creating an excessive length-to-depth ratio for the element. The modulus was found from scaling the element modulus for the planar model to the actual main-arc cell combination based on equivalence of steel area. The combined main cell and arc consisted of approximately 170 PS-32 sheet piles with each pile having an area of 11.8 in<sup>2</sup>. The total pile area is 2,006 in<sup>2</sup> or about 14 ft<sup>2</sup>. The length represented by an arc and main cell is approximately 65 ft, giving a unit steel area of 0.22 ft<sup>2</sup>/ft. The corresponding unit steel area for the two 1-ft-thick elements is 2 ft<sup>2</sup>/ft. To compensate for the greater area in the planar model, the modulus must be multiplied by a factor of 0.11. Assuming a modulus for steel of  $29 \times 10^6$  psi, the element modulus should be  $3.19 \times 10^6$  psi, or approximately  $4.6 \times 10^8$  psf.

### Hoop stiffness spring elements

50. The spring stiffness is determined by assigning values that would make the response of the planar cell to an internal radial pressure equivalent to the response of a circular cell. If a circular cell is subjected to a uniform internal pressure, its radial displacement  $u$  is given by:

$$u = \frac{P \times R^2}{E \times t} \left( 1 - \frac{1}{2} \nu \right) \quad (32)$$

where

$P$  = radial pressure inside cell

$R$  = cell radius

$t$  = cell-wall thickness

which gives an equivalent spring stiffness of:

$$\underline{K} = \frac{P}{u} = \frac{Et}{R^2 \left(1 - \frac{1}{2}v\right)} \quad (33)$$

where  $\underline{K}$  represents a uniformly distributed radial spring acting to restrain radial movement. The planar structure is to be represented by two cell walls connected by discrete springs. The total effect of the springs in resisting lateral movement over a vertical distance  $H$  is:

$$K_s = \frac{P}{\bar{\delta}} \quad (34)$$

where  $\bar{\delta}$  is the lateral movement of the wall and  $p$  is the resultant force  $PH$ . The relationship between the radial displacement of the circular cell and the lateral movement of the two walls is  $\bar{\delta} = 2u$ . Thus, to obtain the equivalent displacement for a given pressure:

$$K_s = \frac{1}{2} \underline{K} H \quad (35)$$

For the example considered by Peters et al. (1986), the stiffness  $\underline{K}$  can be determined from the sheet-pile properties;  $E = 29 \times 10^6$  psi,  $v = 0.3$ , and  $t = 0.5$  in., and cell diameter  $2R = 52$  ft, to get

$$\underline{K} = 3.03 \times 10^5 \text{ pcf}$$

which gives a planar spring stiffness of:

$$K_s = 1.51 \times 10^5 \cdot H \text{ pcf} \quad (36)$$

where  $H$  is the vertical spring spacing.

51. The spring constant derived above was based on the assumption that the effective modulus of the sheet piling was equal to that of a steel membrane having a thickness  $t$ . In fact, displacement of the interlocks reduces the modulus in the tangential (horizontal) direction. To account for interlock behavior, the modulus is multiplied by an "E ratio" which is defined as the ratio of the effective modulus to the modulus of solid steel. An E ratio of 0.03 has been found from experience (Clough and Kuppusamy 1985) to yield a reasonably good correspondence between model and field behavior. Thus the spring modulus used in the above example should be:

$$K_s = 4.5 \times 10^3 \cdot H \text{ pcf} \quad (37)$$

In addition to determining a correct spring constant, it is also necessary to relate the spring force to the interlock stress. The strain in the circular cell is given by:

$$\varepsilon = \frac{u}{R} = \frac{P \times R}{E \times t} \left( 1 - \frac{1}{2} \nu \right) \quad (38)$$

Ignoring the strain in the axial direction, the horizontal stress is given by  $\sigma = E\varepsilon$ . The horizontal force per unit length of interlock is  $T = \sigma_t$ . The unit interlock force is therefore given by:

$$T = P \times R \left( 1 - \frac{1}{2} \nu \right) \quad (39)$$

$$= 0.85 P \times R \quad (40)$$

Following a similar line of reasoning, the spring force  $T_s$  can be related to the displacement by  $T_s = 2K_s u$  and to the interlock force by  $T = T_s/H$ . Therefore by substituting  $\underline{K} = K_s/H$ , the equivalence between  $T$  and  $T_s$  can be developed as follows:

$$\frac{T_s}{H} = \underline{K}u \quad (41)$$

$$= \left[ \frac{E \times t}{R^2 \left( 1 - \frac{1}{2} \nu \right)} \right] \times \left[ \frac{P \times R^2 \left( 1 - \frac{1}{2} \nu \right)}{E \times t} \right] \quad (42)$$

$$= P \quad (43)$$

$$= 1.18 \left( \frac{T}{R} \right) \quad (44)$$

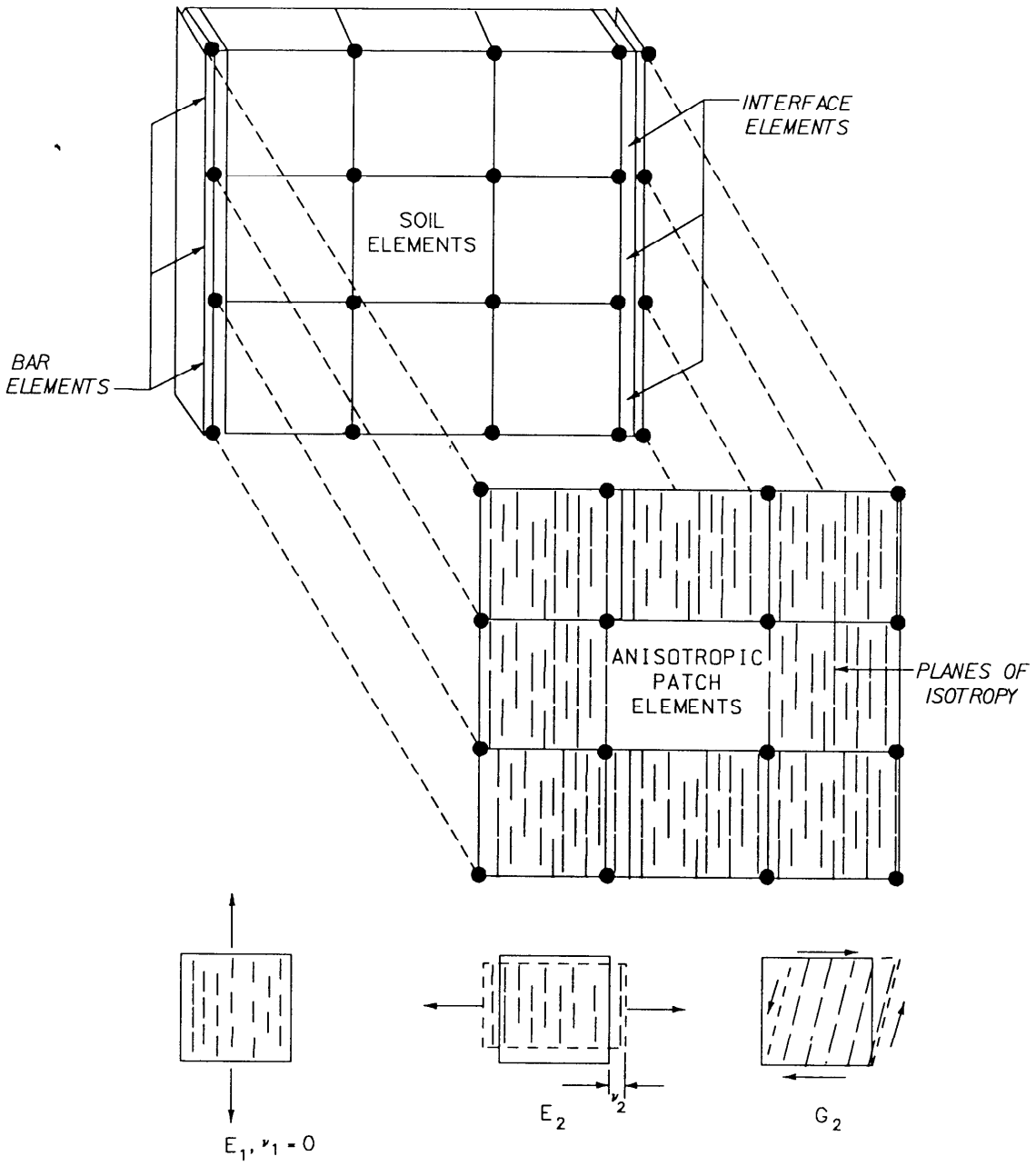


Figure 7. Common-wall model (Peters, Holmes, and Leavell 1986)

Thus, in this example the unit interlock force is related to the spring force by:

$$T = 0.85 \frac{T_s R}{H} \text{ lb/ft} \quad (45)$$

### Alternative description of common-wall elements

52. The common wall sheet piles separating the main and arc cells provide shear resistance that is not conveniently accounted for when modeled using spring elements. To better approximate shear stiffness of the common wall, the soil elements can be overlain with “patch elements” which act independently of the soil except where attached at the outside walls (Peters, Holmes, and Leavell 1986). Figure 7 gives a graphical description of how this technique is implemented. The bar elements account for the higher proportion of steel area in the outside wall, providing additional axial stiffness without contributing to flexural or shear stiffness. The interface elements model the friction between the soil and outside sheet-pile wall, as in the spring model.

53. The patch elements are characterized as a transversely isotropic material acting under plane stress conditions. Five material properties are required to define their behavior. These properties are:  $E_1$  and  $\nu_1$ , which are associated with the common-wall’s axial behavior and  $E_2$ ,  $\nu_2$ , and the shear modulus  $G_2$ , which define stiffness in the tangential direction. The subscripts follow the convention used by Zienkiewicz (1977). These properties allow not only the shear stiffness to be modeled but also the difference between the vertical and horizontal stiffness of the cell. Note that  $\nu_1$  does not appear in the plane stress stiffness formulation and  $\nu_2$  can be set to equal zero to simplify property determination. In fact, the interlocks may tend to inhibit the Poisson’s effect, although no data exist to support this assumption. Provisions have been made in the finite element code for  $\nu_2$  and values other than zero could be included.

### Development of anisotropic properties

54. The rationale for estimating the stiffness properties follows the same line of reasoning outlined previously: the various components of stiffness can be uncoupled and treated independently. The reasoning for each parameter is described as follows:

55.  $E_2$ . The equation for determining the hoop stiffness  $E_2$  is derived by relating the response of a vertical planar slice through the center of the cell to that of a circular cell. Subjecting a circular cell to a uniform internal pressure, its radial displacement  $u$  is given by:

$$u = \frac{P \times R}{E_s t} \left( 1 - \frac{1}{2} \nu \right) \quad (46)$$

where

$E_s$  = Young's modulus of steel

$\nu$  = Poisson's ratio, assumed to equal 0.0

The lateral displacement  $\delta$  caused by the same pressure in the planar slice is given by:

$$\bar{\delta} = \frac{\bar{P} \times d \times L}{E_2 \bar{t}} \quad (47)$$

where ,

$\bar{P}$  = lateral pressure

$d$  = unit thickness of slice

$E_2$  = hoop stiffness or, equivalently, the effective modulus of the slice

$\bar{t}$  = slice thickness (= 1)

$L$  = slice length

Substituting  $\bar{\delta} = 2u$  ,  $L = 2R$  , and  $\bar{P} = P$  into Equation 47 and equating Equations 46 and 47, it is found that

$$E_2 = \frac{E_s \times t}{R} \quad (48)$$

Solving Equation 48 with the following variable values ( $E_s = 4.18 \times 10^9$  psf ,  $t = 0.0667$  ft , and  $R = 25$  ft) results in a hoop stiffness of  $E_2 = 1.12 \times 10^7$  psf .

Because of displacement in the sheet-pile interlocks,  $E_2$  is multiplied by an "E ratio" of 0.03, giving

$$E_2 = 3.34 \times 10^5 \text{ psf}$$

56. The procedure outlined above is clearly equivalent to that used to determine the horizontal spring stiffness in the conventional planar model. If  $E_1$  and  $G_2$  are set to zero, the patch elements behave as a continuous spring.

57.  **$E_1$  and  $G_2$**  . The vertical stiffness  $E_1$  is obtained by determining the percent steel in a typical planar section of the sheet pile wall and adjusting the modulus of steel to obtain an equivalent stiffness. Using the total length of sheet pile material as 240 ft, an average thickness of 0.0667 ft, and a total area of 3,176 ft<sup>3</sup>, the percent steel in a section of wall is approximately 0.51 percent. Multiplying the modulus of steel,  $4.18 \times 10^9$  psf, times 0.51 percent gives

$$E_1 = 2.13 \times 10^7 \text{ psf}$$

The shear modulus  $G_2$  is assumed to be 0.4 of  $E_1$ , making

$$G_2 = 8.52 \times 10^6 \text{ psf}$$

The 0.4 multiplier accounts for the Poisson's ratio of the steel within the pile web. The present model does not account for slip along the interlocks which would tend to reduce the shear stiffness.

### **Axial bar stiffness**

58. The axial bar placed along the outer walls accounts for the fact that the area of steel at those locations is the same in both the prototype and the planar slice. The area of steel computations for the bar stiffness is identical to that described for the solid wall elements in previous sections of the report.

## PART IV: USE OF SOILSTRUCT PROGRAM

### Sign Convention and Coordinate System

59. All input data and results are specified using a right-hand coordinate system; the x-axis being horizontal and positive to the right and the y-axis being vertical and positive upwards. The sign convention for stresses acting at the center of a two-dimensional element is shown in Figure 8a. Compressive stresses are taken to be positive.

60. Stresses for interface elements are defined with respect to their local axes along the length of the interface  $x'$  as defined by the I and J nodes, and normal to the element  $y'$  as shown in Figure 8b. Positive normal stresses are compressive. Positive shear stresses act in the positive  $x'$  direction along the length of the interface as shown in Figure 8b.

61. Positive forces are taken to be compressive in all one-dimensional bar elements, with the exception of bar reinforcement elements. For these elements, positive forces are taken to be tensile.

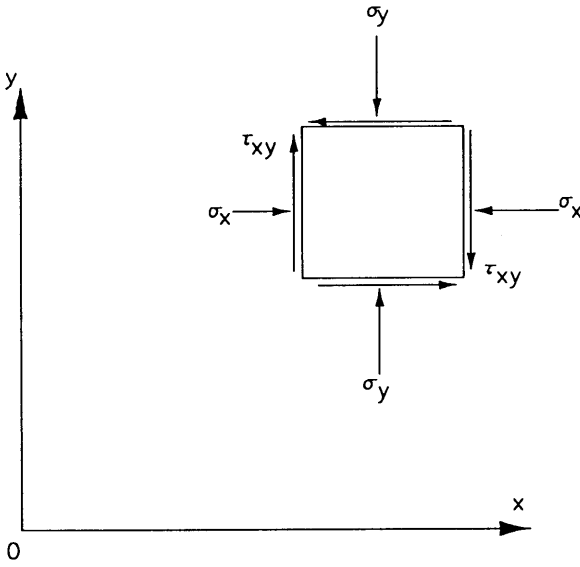
### Units

62. Any consistent set of units can be used with SOILSTRUCT, with one cautionary note. The normal stiffness of interface elements is arbitrarily set to a value of  $1 \times 10^8$ , independent of units, as discussed in paragraph 33.

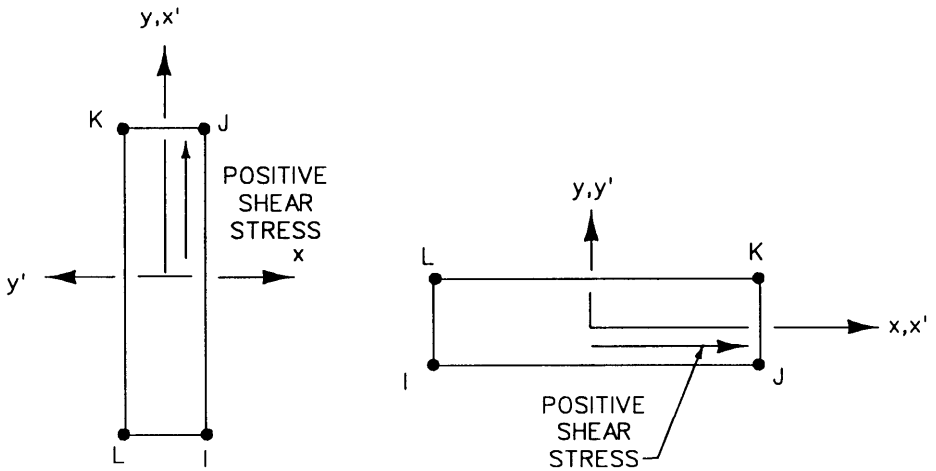
### Capacity

63. The capacity of the program is determined by the size of variables in the common block and dimension statements. The global stiffness matrix [K] is stored within the program in vector SN. The dimension of SN is equal to 1,600,000, and the maximum number of either nodes or two-dimensional elements is 4,000. The dimensions for all of the arrays are given throughout the input guide. Double precision is specified for all arrays in the CRAY Y-MP version of SOILSTRUCT.

64. The global stiffness matrix is assembled in vector form using a modified skyline procedure. Therefore, there is no direct correlation between the size of SN and the maximum number of nodes or elements. If the required size of SN exceeds 1,600,000 during execution of SOILSTRUCT, the program will terminate execution and print the size required for the SN vector. If this occurs, two statements must be modified within the computer code; (a) the dimension of the SN vector, found in the main program, must be increased to the required value, and (b) a call statement, comparing the required size of the SN vector for the problem being analyzed to the actual dimension of SN, must be revised in subroutine DETNA.



a. *Coordinate system and sign convention for positive stresses for two-dimensional elements*



b. *Definition of interface local axes and sign convention for positive shear stress*

*Figure 8. Sign conventions and coordinate axes for stress and displacements (Clough 1984)*

## REFERENCES

- Clough, G. W. 1984. "User's Manual for Program SOILSTRUCT," Virginia Polytechnic Institute and State University, Blacksburg, VA.
- Clough, G. W., and Duncan, J. M. 1969 (Sep). "Finite Element Analyses of Port Allen and Old River Locks," Report No. TE 69-3, College of Engineering, Office of Research Services, University of California, Berkeley, CA.
- Clough, G. W., and Kuppusamy, T. 1985. "Finite Element Analysis of Lock and Dam 26 Cofferdam," *Journal of Geotechnical Engineering Division, American Society of Civil Engineers*, Vol III, No. 4, pp 521-541.
- Clough, G. W., and Tsui, Y. 1977. "Static Analysis of Earth Retaining Structures," *Numerical Methods in Geotechnical Engineering*, C. S. Desai and J. T. Christian, eds., McGraw-Hill Book Company, New York, pp 506-527.
- Doherty, W. P., Wilson, E.L., and Taylor, R. L. 1969. "Stress Analysis of Axisymmetric Solids Utilizing Higher-Order Quadrilateral Finite Elements," Report No. SESM 69-3, Structural Engineering Laboratory, University of California, Berkeley, CA.
- Duncan, J. M., Byrne, P., Wong, K. S., and Mabry, P. 1978 (Apr). "Strength, Stress-Strain and Bulk Modulus Parameters for Finite Element Analyses of Stresses and Movements in Soil Masses," Report No. UCB/GT/78-02, College of Engineering, Office of Research Services, University of California, Berkeley, CA.
- Duncan, J. M., and Chang, C. Y. 1970 (Sep). "Nonlinear Analysis of Stress and Strain in Soils," *Journal of the Soil Mechanics and Foundations Division, ASCE*, Vol 96, No. SM5, Proc. Paper 7513, pp 1629-1653.
- Duncan, J. M., Seed, R. B., Wong, K. S., and Ozawa, Y. 1984 (Nov). "FEADAM84: A Computer Program for Finite Element Analysis of Dams," Research Report No. SU/GT/84-03, Geotechnical Engineering, Department of Civil Engineering, Stanford University, Palo Alto, CA.
- Dunlap, P., Duncan, J. M., and Seed, H.B. 1968 (May). "Finite Element Analyses of Slopes in Soil," Contract Report S-68-6, US Army Engineer Waterways Experiment Station, Vicksburg, MS.
- Goodman, R. E., Taylor, R. L., and Breeke, T. L. 1968. "A Model for the Mechanics of Jointed Rock," *Journal of the Soil Mechanics and Foundations Division, ASCE*, No. SM3.
- Jaky, J. 1948. "Pressure in Silos," *Proceedings, 2nd International Conference on Soil Mechanics and Foundation Engineering*, Vol 1, pp 103-107.
- Leavell, D. A., Peters, J. F., Edris, E. V., and Holmes, T. L. 1989. "Development of Finite-Element Based Design Procedure for Sheet-Pile Walls," Technical Report GL-89-14, US Army Engineer Waterways Experiment Station, Vicksburg, MS.
- Mana, A.I. 1978. "Finite Element Analyses of Deep Excavation Behavior in Soft Clay," Ph.D. dissertation submitted to the Department of Civil Engineering and the Committee on Graduate Studies, Stanford University, Palo Alto, CA.
- Mosher, R. L., and Knowles, V. R. 1990. "Finite Element Study of Tieback Wall for Bon-neville Navigation Lock," Technical Report ITL-90-4, US Army Engineer Waterways Experiment Station, Vicksburg, MS.
- Peters, J. F., Holmes, T. L., and Leavell, D. A. 1986. "Finite Element Analysis of William-son CBD Sheetpile Cell Floodwall, TASK 1," letter report to Department of the Army COE, Huntington District, Huntington, WV.

- Peterson, M. S., Kulhawy, F. H., Nucci, L. R., and Wasil, B. A. 1976. "Stress-Deformation Behavior of Soil-Concrete Interfaces," Contract Report B-49, Department of Civil Engineering, Syracuse University, Syracuse, NY.
- Potyondy, J. G. 1961 (Dec). "Skin Friction Between Various Soils and Construction Materials," *Geotechnique*, Vol II, No. 4, pp 339-353.
- Timoshenko, S. and Woinowsky-Krieger, S. 1959. *Theory of Plates and Shells*, 2nd ed., McGraw-Hill Book Company, New York, p 5.
- Zienkiewicz, O. C. 1977. *The Finite Element Method*, 3rd ed., McGraw-Hill Book Company, New York.

**Input Data Sequence**

The format of the input data is free-field format unless stated otherwise.

**1. IDENTIFICATION CARD — FORMAT (20A4)**

<u>Column</u>	<u>Variable</u>	<u>Explanation</u>
1-80	HED	Analysis identification.

**2a. DATA CONTROL CARD**

All nodes and two-dimensional and interface elements to be used in the analysis must initially be included in the mesh; additions or deletions of these elements are not allowed, but the material parameters can be changed to make them inactive. One-dimensional bar elements may initially be included in the mesh or added in subsequent construction steps.

<u>Variable</u>	<u>Explanation</u>
NUMNP	Number of nodal points (4,000 maximum).
NUMEL	Number of elements initially in the mesh, excluding bar and beam elements, but including interface elements. NUMEL, then, includes NUMJT (4,000 maximum). Interface elements should be numbered first.
NUMJT	Number of interface elements (400 maximum).
NUMBER	Number of bar elements initially in the mesh, including those bar elements added in subsequent construction stages (400 maximum). NUMBER also includes NSTRAN, the number of bar elements used as strain gages (see card number 2c).
NC	Number of loading and construction steps (40 maximum).
NMOD	Modulus specification code- = 0 if modulus calculation codes input with loading information card. = 1 if modulus calculation codes input with modulus calculation card.

Variable	Explanation
INIT	<p>Initial stress input code -</p> <p>= 0 if external input from cards or tape, included in input.</p> <p>= 1 if internally generated from gravity turn-on analysis.</p> <p>= 2 if initial stresses and displacements are to be set equal to zero within SOILSTRUCT.</p> <p>If INIT <math>\neq</math> 0 or <math>\neq</math> 1 or <math>\neq</math> 2 , initial stresses are generated assuming a horizontal ground surface, horizontal water table, and <math>\sigma_x = K_o \sigma_y</math> .</p>
KI	<p>Interface element activation code -</p> <p>= 0 not activated during initial stress computation.</p> <p>= 1 activated during initial stress computation.</p> <p>KI is used when INIT = 0 . If INIT = 0 , then KI can be set equal to zero.</p>
IHORIZ	<p>Ground surface inclination code -</p> <p>= 0 horizontal ground surface. Vertical stresses are computed using a gravity turn-on method of analysis. Horizontal stresses are computed assuming <math>K_o = \nu/(1- \nu)</math> unless <math>K_o</math> is specified.</p> <p>= 1 sloping ground surface. Vertical and horizontal stresses are calculated from a gravity turn-on analysis assuming linear elastic response of soil - i.e., <math>K_o = \nu/(1- \nu)</math> .</p>
ITRD	<p>Analysis printout code -</p> <p>= 0 if initial stresses and results of the final iteration are to be printed.</p> <p>= 1 if initial stresses and results of <b>all</b> iterations are to be printed.</p> <p>= 2 if initial stresses are <b>not</b> printed but results of <b>all</b> iterations are to be printed.</p> <p>= 3 if initial stresses and results of the final iteration are to be printed. No substep results are to be printed.</p> <p>= -2 if initial stresses are <b>not</b> printed but results of the <b>final</b> iteration are to be printed.</p>
ILIST	<p>Element and nodal point card data printout code -</p> <p>= 0 if not printed.</p> <p>= 1 if printed.</p>

<u>Variable</u>	<u>Explanation</u>
IPUNCH	Restart file code - = 0 if no restart file is to be generated. = 1 if a restart file is to be generated. Only the results of the final iteration are used.
ITAPE	Disk storage code - = 0 if no disk storage. = 1 if storage of displacements from final iteration. = 2 if storage of all data except displacements from final iteration.
GAMW	Unit weight of water.
PATM	Atmospheric pressure.

The unit weight of water and the atmospheric pressure are included as basic parameters. Either English or SI units can be used. All data must be compatible with input coordinate, pressure, and material property parameters.

## 2b. MATERIAL ALLOCATION CARD

All two-dimensional material types are assigned material numbers first, followed by the interface material types. Bar elements are not assigned a material type number, but are identified solely by their element number. If a number for NATYP, or NA2TYP, for example, is not required, assign a value of zero.

<u>Variable</u>	<u>Explanation</u>
NUMMAT	Total number of material types, including both two-dimensional soil or construction material types and interface material types.
NUMSOL	Total number of material types excluding the interface material types. Thus, (NUMMAT-NUMSOL) must equal the number of interface material types.
NATYP	Material type number assigned to elements initially having the properties of air. Usually, elements that will be built are initially identified as air elements.
NCTYP	Structural material type, such as concrete or sheet-piling.
NB1TYP	Backfill material type 1. (Refer to section 13b on fill or concrete placement.)
NB2TYP	Backfill material type 2. (Refer to section 13b on fill or concrete placement.)

<u>Variable</u>	<u>Explanation</u>
NSTRAN	Number of bar elements used as strain gages. These bar elements are numbered first.
NOMOM	Number of <b>pairs</b> of bar element strain gages used in moment computations (see paragraph 42).
EBAR*	Young's modulus for steel reinforcement. Used in conjunction with bar element strain gages.
EBEND*	Young's modulus for the bending member. Used in conjunction with bar element strain gages and moment computations.
NA2TYP	Material type number assigned to interface elements having the properties of air.
R_FILL	Total number of soil element material types in which layers of reinforcement are present. When conducting a restart analysis in which reinforcement is present, specify a negative value for R_FILL.
	If any of the above are not needed, enter zero.

---

\* Set equal to  $E_e$  for sheet piles (see paragraph 41).

## 2c. CALCULATION PROCEDURES

These five integers activate special features incorporated within this version of SOILSTRUCT.

Variable	Explanation
KEYEI	<p>Procedure used to define the parameter <math>M_B</math> and the shear modulus <math>M_D</math> of the stress-strain matrix <math>[D]</math> where <math>\{\sigma\} = [D]\{\epsilon\}</math>.</p> $[D] = \begin{bmatrix} (M_B + M_D) & (M_B - M_D) & 0 \\ (M_B - M_D) & (M_B + M_D) & 0 \\ 0 & 0 & M_D \end{bmatrix}$ <p>= -1, then  <math>M_B = M_B(E_i, \nu)</math>  <math>M_D = M_D(E_t, \nu)</math></p> <p>= 0, then  <math>M_B = M_B(E_t, B)</math>  <math>M_D = M_D(E_t, B)</math></p> <p>= 1, then  <math>M_B = M_B(E_i, B)</math>  <math>M_D = M_D(E_t, B)</math></p>
IPETER	<p>Procedure used to calculate the stress level, SL (see Figure 2).</p> <p>= 0 when SL is calculated using  <math>(\sigma_3)_{failure} = (\sigma_3)_{current}</math></p> <p>= 1 when SL is calculated using mean pressure at failure equal to current mean pressure.</p>
NPETER	<p>Procedure used to update the total interface nodal point displacements.</p> <p>= 0 if I, J, K, and L interface node displacements are updated.</p> <p>= 1 if interface node displacements I and L are set equal, and node displacements J and K are set equal. This option is used for new interface elements placed adjacent to pre-existing structural elements.</p>

KEYH2O	Procedure used to define the lateral stress within newly placed fill elements (see card group 13b). = 0 when $\sigma_x = K_o \sigma_y$ = 1 when $\sigma_x = \sigma_y$
KEYSEP	Applied seepage forces (see card group 13c). = 0 if lateral and vertical seepage forces are to be applied. = 1 if only <b>vertical</b> seepage forces are to be applied.

### 3. LOADING INFORMATION CARD

One card is supplied for each load step. One to three load/ construction modes can be included in each load step. The load or construction mode codes include:

<u>KCS(NC,I)</u>	<u>DESCRIPTION</u>
1	Excavation (equivalent nodal loads can be applied in equal increments).
2	Fill placement (subroutine SUBSTP cannot be used in conjunction with the fill placement procedures of subroutine BUILD).
3	Seepage loading (equivalent nodal loads can be applied in equal increments).
4	Deletion of bar element (force in the element can be applied in equal increments).
5	Installation of bar element (prestress force can be applied in equal increments).
6	Boundary pressure loading (equivalent nodal loads can be applied in equal increments).
7	Temperature loading (the total temperature change can be applied in equal increments).
8	Support displacement (the total displacement can be applied in in equal increments).
9	Concentrated nodal loads (can be applied in equal increments).
10	Element material type change.

As indicated in the listing, prescribed loads, displacements, or temperature changes can be analyzed in equal increments, or substeps, for each load case. Subroutine SUBSTP generates the equivalent load increments, then main analyzes all increments prior to analyzing the next load step. With one exception, all loading/construction modes that can be applied in increments, or substeps, can also be applied in any combination in any

load step. The number of substeps, however, will be the same for all loading or construction modes included in the load step. The exception is temperature loading; if a temperature change is specified, and a given number of substeps are specified, then only the corresponding temperature loads can be specified in the loading step - i.e.,  $KCS(N,2)$  and  $KCS(N,3)$  must be set equal to zero. If the number of substeps,  $NSBSP$ , is equal to zero, then temperature loading can be included with other loading/construction modes in a load step.

Since the same input format is used in modes 8 and 9, the following rules apply; if only concentrated nodal loads are specified, use mode 9, if only support displacements are specified, use mode 8, and if both loads and displacements are specified, use mode 8.

<u>Variable</u>	<u>Explanation</u>
$KCS(NC,1)$	First loading/construction mode code.
$KCS(NC,2)$	Second loading/construction mode code.
$KCS(NC,3)$	Third loading/construction mode code.
	$KSC(NC,1)$ , $KCS(NC,2)$ , and $KCS(NC,3)$ can be input in any numerical order, but the modes are processed in ascending numerical order: If the second and/or third loadings are not required, then $KCS(NC,2)$ $KCS(NC,3)$ should be set equal to zero.
$NUMIT(NC)$	Number of iterations for the load step. $NUMIT(NC)$ applies to <b>each</b> substep if substeps are specified. $NUMIT(NC) = 0$ is the same as $NUMIT(NC) = 1$ .
$NUMSS(NC)$	Number of substeps, the minimum value which may be assigned to $NUMSS(NC)$ is one.
$MOD(1,NC)$	Modulus calculation code- = 1 if a loading modulus is to be calculated. = 2 if an unload-reload modulus is to be calculated. = 0 if the computer is to decide the type of modulus to be calculated. In this case, if the most recently calculated maximum shear stress for an element is less than all previous values of maximum shear stress, an unload-reload modulus is assigned. Otherwise a primary loading modulus is assigned.

Additional input is required here only if  $NMOD = 0$ . All material types, other than interface or bar elements, are given one of the above codes. If  $NMOD = 0$  and  $NC = 0$ , as might be the case

for an analysis of initial stresses, MOD(I,1) is set equal to zero, or the computer decides.

IPRT(NC)	= 0 Do not print the force vector. = 1 Print the force vector.
IPLT(NC)	= 0 Do not create a plot file. = 1 Create a plot file, including moments. = 2 Create a plot file of moments only. = 3 Create a NISA plot file of geometry, displacements, and stresses.
HEDCS(NC)	Description of the load step.

#### 4. MODULUS SPECIFICATION CARD

This card is required only if NMOD = 1 and NC = 0 . A card is required for each loading step, 1 to NC . In this option, values of the modulus specification code are specified for each material type (and thus each element, excluding bar and interface elements), regardless of the change in maximum shear strain that may have occurred.

<u>Variable</u>	<u>Explanation</u>
MOD(I,NC)	Modulus calculation code for each material type (1 to NUMSOL) for the first load step. Separate cards are required for each load step.

#### 5. MATERIAL PROPERTY CARDS

These pairs of cards are used only to define the material properties for two-dimensional elements, excluding bar and interface material types. The first and second lines are supplied in order of material type number N = 1 to NUMSOL . Information or properties not required for a material type can be set equal to zero.

<u>Variable</u>	<u>Explanation</u>
GUI(N)	Poisson's ratio before failure, or the bulk modulus number $K_b$ .
GUF(N)	Poisson's ratio at failure (no greater than 0.49), or the bulk modulus exponent, m .
GAM(N)	Total or buoyant unit weight (always specified, regardless of drained or undrained material behavior).
FR(N)	The failure ratio $R_f$ .
AO(N)	Coefficient of lateral earth pressure at rest $K_o$ as pertaining to effective stresses.

Variable	Explanation
PHI(N)	Friction angle in degrees. If IDRAIN = 2 , PHI should be set equal to zero.
XXP(N)	The modulus exponent n . For a linear elastic material n must be set equal to 0. For saturated soils when PHI(N) = 0. , n is normally set equal to 0.00001.
IDRAIN(N)	Material behavior code - = -1 if patch element = 0 if undrained = 1 if drained = 2 if value entered for cohesion is equal to the ratio $(S_u/p'_c)$ ,  where $p'_c = 1/2 (\sigma'_{1c} + \sigma'_{3c})$ .
HCOEF(N)	The modulus number K .
ULCOEF(N)	The unload-reload modulus number $K_{ur}$ .
COHE(N)	Undrained shear strength or cohesion. When IDRAIN(N) = 2, COHE(N) is set equal to the normalized strength ratio $(S_u/p'_c)$ .
E(N)	Tangent modulus at failure for isotropic, nonlinear materials, or Young's modulus for elastic materials.
ALPHA(N)	Coefficient of linear thermal expansion for structural element. For non-structural material types, set ALPHA(N) equal to zero.
EIMN(N)	Minimum initial tangent modulus for isotropic, nonlinear materials. Set EIMN(N) equal to zero for elastic materials.
TENS(N)	Minimum allowable value of the minor principal stress for isotropic, nonlinear materials. If tensile, input TENS(N) as a negative value. For elastic materials, set equal to zero.

The variables described above correspond to typical soil materials. However, according to the value given to IDRAIN these parameters may take on different meanings. The table below gives the interpretation given to each variable for each value of IDRAIN . Note that \* implies that the variable is not used but a value of 0.0 should be inserted as a “place holder” to insure other values are read properly.

Variable	Explanation
----------	-------------

IDRAIN = 0 (Total stress “undrained” specification)

GUI	GUI (.49+)
GUF	*
GAM	GAM (total)
FR	FR
AO	$K_o$ (drained)
PHI	PHI (total)
XXP	XXP (> 10e - 5)
IDRAIN	0
HCOEF	HCOEF
ULCOEF	ULCOEF
COHE	COHE (total)
E	*
ALPHA	ALPHA
EIMN	EIMN
TENS	TENS

IDRAIN = 1 (Effective stress specification)

GUI	GUI or $K_b$
GUF	GUF or m
GAM	GAM (bouyant if below water table)
FR	FR
AO	$K_o$ (drained)
PHI	PHI (effective)
XXP	XXP
IDRAIN	1
HCOEF	HCOEF
ULCOEF	ULCOEF
COHE	COHE (effective)
E	*

Variable	Explanation
ALPHA	ALPHA
EIMN	EIMN
TENS	TENS

IDRAIN = 1 (Elastic materials; used for MTYPE = NCTYP OR NATYP )

GUI	GUI or $K_b$
GUF	*
GAM	GAM
FR	*
AO	$K_o$ (drained)
PHI	*
XXP	0
IDRAIN	0 or .1
HCOEF	*
ULCOEF	*
COHE	*
E	E
ALPHA	ALPHA
EIMN	*
TENS	*

IDRAIN = 2 (Undrained with properties based on initial consolidation stress)

GUI	GUI (= .49+)
GUF	*
GAM	GAM (Total above water table & buoyant below)
FR	FR
AO	$K_o$ (drained)
PHI	PHI (O.)
XXP	XXP (small but $> 10e - 5$ )
IDRAIN	2
HCOEF	$E_t/S_u$
ULCOEF	$E_u/S_u$

Variable	Explanation
COHE	$S_u/p_c$
E	*
ALPHA	*
EIMN	EIMN
TENS	TENS/ $S_u$

IDRAIN = -1 (Anisotropic "patch" elements used to model sheet pile cells)

GUI	$v_2$
GUF	*
GAM	*
FR	*
AO	*
PHI	$E_1/E_2$
XXP	$G_2/E_2$
IDRAIN	-1
HCOEF	*
COHE	*
E	$E_2$
ALPHA	*
EIMN	*
TENS	*

## 6. INTERFACE PROPERTY CARD

One card is supplied for each interface material type,  $N = 1$  to NUMJT . If no interface elements are used, no cards are required. RKN (N) is set equal to  $1 \times 10^8$  (or = 1 if air interface element) within the code.

Variable	Explanation
PHJ(N)	Interface friction angle in degrees.
RKS(N)	The minimum value for the interface shear stiffness $k_s$ .
COJ(N)	Interface cohesion $c$ .
FRJ(N)	Failure ratio $R_{fi}$ .

Variable	Explanation
TENSJ(N)	Tensile strength of interface $\sigma_t$ .
IADJMT(N)	Adjacent two-dimensional element material type number.
RKJ(N)	The interface modulus number $K_j$ .
XXPJ(N)	The interface modulus exponent $n_i$ .

## 7. NODAL POINT CARDS — FORMAT (I10, 4D10.4)

One card is supplied for each node. The numbering of nodal points must be sequential and the input for some of the nodes can be omitted. Those nodes omitted are automatically generated by the program at equal spacings between those nodes specified. The first and last nodes must always be specified. Note that DP(N) and PP(N) are automatically generated in equal increments for those nodes omitted (see Figure A1).

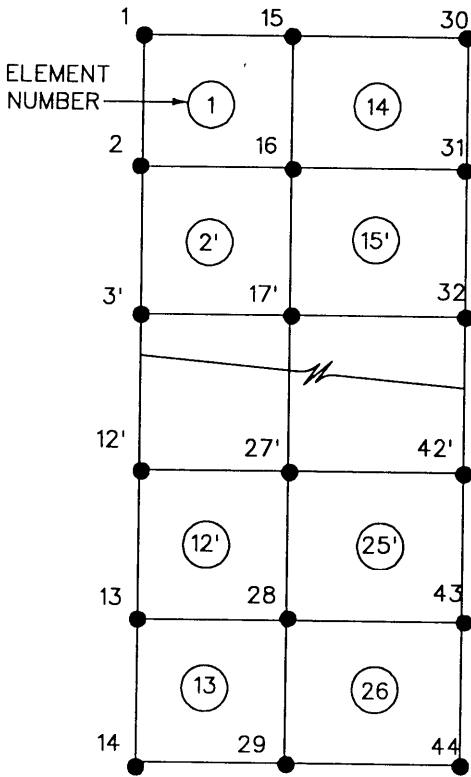
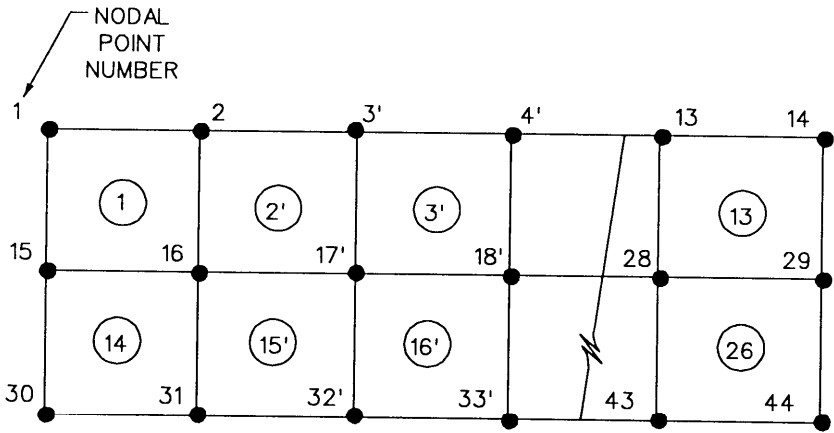
Column	Variable	Explanation
1-10	N	Nodal point number.
11-20	X(N)	X coordinate, positive to right.
21-30	Y(N)	Y coordinate, positive upward.
31-40	PP(N)	Pore pressure in head of water; zero or blank if not specified. Pore pressure must be specified for drained materials but not for undrained materials.
41-50	DP(N)	Change in pore pressure in head of water for soil elements; change in temperature for linear elastic structural material, otherwise set equal to zero.

## 8. BOUNDARY CONDITION CARDS

Cards 1 through 8 are supplied as required to specify restraints of boundary nodes. If there are no restrained nodes, then this series of cards is not required. On each card, the constrained nodes must be in sequential order.

### (a) FIRST CARD

Variable	Explanation
NOY	Number of nodal points fixed against Y-movement only.
NOX	Number of nodal points fixed against X-movement only.
NOXY	Number of nodal points fixed against both X- and Y-movement.



PRIMED NUMBERS INDICATE NODE OR ELEMENT NUMBERS GENERATED BY THE COMPUTER, USING THE INPUT (UNPRIMED) NODE AND ELEMENT NUMBERS.

Figure A1. Examples of numbering nodes and elements if generated by the program (Clough 1984)

**(b) SECOND CARD**

<u>Variable</u>	<u>Explanation</u>
IC(N)	Nodal point number of the first nodal point fixed against Y-movement. Additional nodal points fixed against Y-movement, N = 2 to NOY , are specified in the next columns and on additional cards as required.

**(c) THIRD CARD**

<u>Variable</u>	<u>Explanation</u>
IC(N)	Nodal point number of the first nodal point fixed against X-movement. Additional nodal points fixed against X-movement, N = 2 to NOX , are specified in the next columns and on additional cards as required.

**(d) FOURTH CARD**

<u>Variable</u>	<u>Explanation</u>
IC(N)	Nodal point number of the first nodal point fixed against both X- and Y-movement.  Additional nodal points fixed against both X- and Y-movement, N = 2 to NOXY , are specified in the next columns and on additional cards as required.

**9. ELEMENT CARD**

One card is supplied for each two-dimensional element and interface element; bar elements are not included in this series of cards. All interface elements are supplied in sequential order first, followed by two-dimensional elements, also in sequential order. Thus, interface elements must be numbered from N = 1 to NUMJT , and two-dimensional elements from N = (NUMJT + 1) to NUMEL .

Nodal point numbers must be specified consecutively, proceeding counterclockwise around the element, as shown in Figure A2.

The first and last nodal point numbers specified for interface elements must have the same coordinates, as shown in Figure A2. Triangular two-dimensional elements having four different nodal point numbers may not be used; the first and last point numbers of a triangular element must be identical.

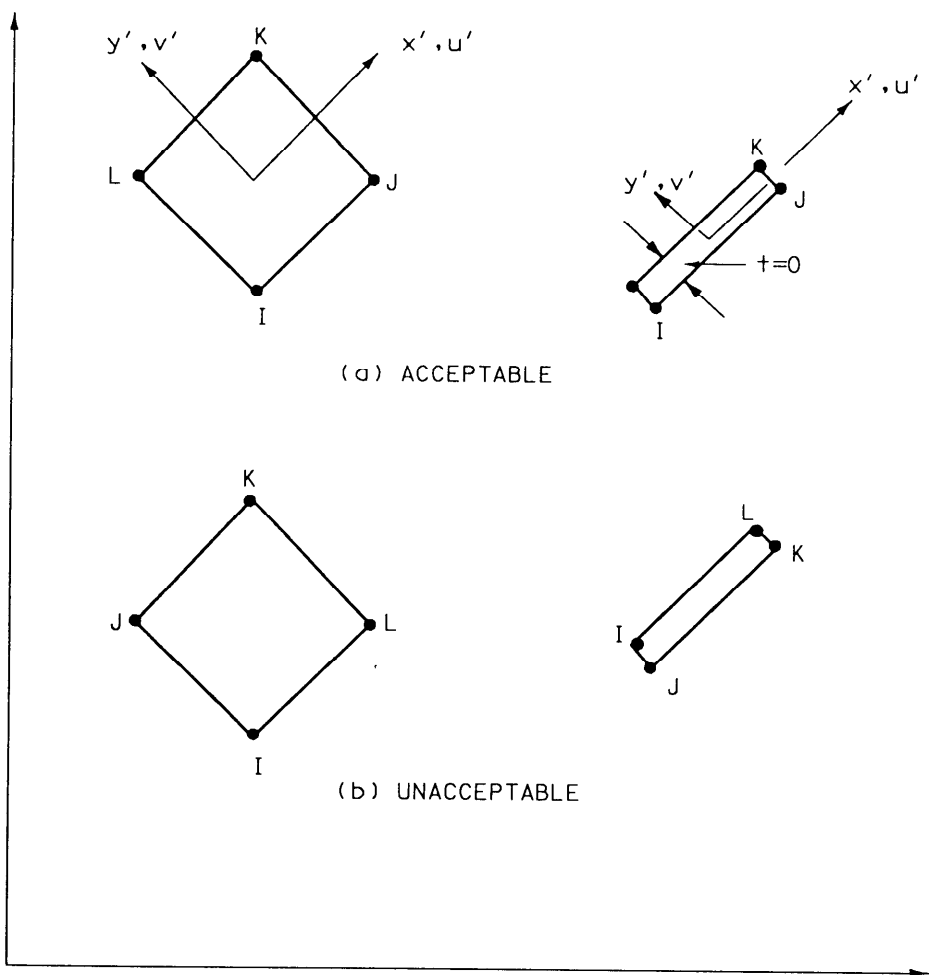


Figure A2. Nodal point numbering of isoparametric QM5 element and interface element (Clough 1984)

Element numbers in a row may be omitted, in which case the omitted elements will be generated by incrementing the element number  $N$  and the nodal point numbers  $I$ ,  $J$ ,  $K$ , and  $L$  by one, and by assigning the same material type number as specified for the last element. The first and last elements in the row must be specified (see Figure A1). If no elements are omitted, the element numbering may be done in any order, provided all interface elements are numbered first.

Variable	Explanation
$N$	Element number.
$IL(N,1)$	Number of nodal point $I$ .
$IL(N,2)$	Number of nodal point $J$ .
$IL(N,3)$	Number of nodal point $K$ .

Variable	Explanation
IL(N,4)	Number of nodal point L .
IL(N,5)	Material type number.

## 10. BAR ELEMENT CARD

One card is supplied for each bar element initially in the mesh or, added during an incremental load step. Note that for a continuation analysis this card is not automatically generated. Elements are numbered sequentially from  $N = 1$  to  $NMBAR$  , with  $NSTRAN$  strain gage bar elements numbered first.

Variable	Explanation
N	Bar element number.
IB(N,1)	Number of nodal point I .
IB(N,2)	Number of nodal point J .
IB(N,3)	Spring response type code - = 1 if both compression and tension of bar allowed. = 2 if only compression allowed. = 3 if only tension allowed.
BAR(N,1)	$\cos \alpha$
BAR(N,2)	$\sin \alpha$  The sign convention of angle $\alpha$ is determined as shown in Figure A3. Angle $\alpha$ is measured counter-clockwise from a line drawn in the positive x-direction, originating at node I and connecting node I to node J .
BAR(N,3)	Prestress force in the bar element. The force must be prescribed at both node I and node J using a load/construction mode 9 load step.
BAR(N,4)	Stiffness of bar element. This is usually computed as $AE/L$ , but the mesh length (distance from node I to node J ) need not, and usually does not, correspond to the actual length. Set equal to 1.0 for bar elements used as strain gages.
BAR(N,5)	Displacement of bar element at activation. This allows for a specified magnitude of slack at the strut connection; the bar will deform $BAR(N,5)$ prior to its stiffness being activated.

Bar elements can function as either anchors or strut (spring) supports. The required parameters are dependent on the type of bar element specified.

If a **strut support** is specified, nodal point J is a node fixed against x- or y-movement, depending on the orientation of the strut being modeled. For program storage efficiency the number of node J should be as close as possible to the number of node I. Nodal point I represents the point of connection between the wall and the actual strut. Nodal points I and J, then, are not necessarily physically connected, since the element stiffness is input independently. Nodal point J allows the force at the J node to be carried into the system as a reaction at a fixed node. This is consistent with the typical mesh representation of one half of a symmetric excavation. The values of  $\sin \alpha$  and  $\cos \alpha$  are specified according to the sign convention shown in Figure A3. The values are

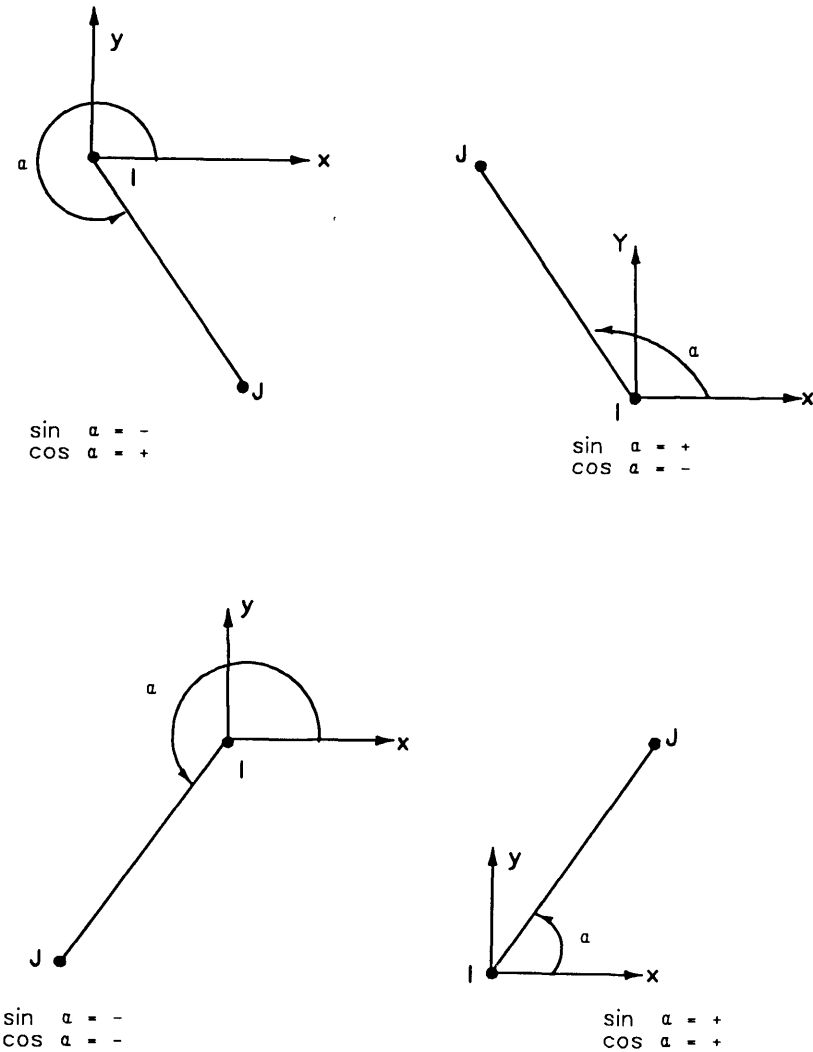


Figure A3. Sign convention and definition of local axes for bar element (Clough 1984)

input to represent the line of action of the strut support, and do not need to correspond to the relative positions of the I and J nodes.

If an **anchor** is specified, nodal points I and J physically represent two ends of the anchor, and must be restrained appropriately. The values of  $\sin \alpha$  and  $\cos \alpha$  must correspond to the relative positions of the I and J nodes representing the ends of the anchor. Stiffness is computed as  $AE/L$ , with L being the distance between nodes I and J, and either A or E altered to give the correct stiffness. Stiffness of an anchor or a strut support is inputted as force per length of wall.

For either element type, **specifying the prestress force does not apply the force**. The concentrated force load/construction mode must be used for this purpose. Thus, bar elements initially in the mesh cannot carry a prestress force, since it is not applied by a gravity turn-on analysis.

## 11. MOMENT COMPUTATION

This input is supplied only if  $NOMOM \neq 0$ . One card is supplied for each pair of bar element strain gages used in moment computations (see Equation 30).

Variable	Explanation
MOMBAR(N,1)	Bar element number for strain gage No. 1.
MOMBAR(N,2)	Bar element number for strain gage No. 2.

This card is repeated for  $N = 2$ ,  $NOMOM$  pairs of bar element strain gages.

## 12. SOIL REINFORCEMENT

This input is supplied only if  $R\_FILL \neq 0$ . This series of cards define the layer geometry and material properties for the reinforcement material placed within a backfill. Each layer of reinforcement is modeled using a series of bar elements. The total number of reinforcement bar elements and coordinates is determined within the computer code. The length of each bar element corresponds to the length of each reinforcement layer that is contained within each two-dimensional soil element. The number of nodal points for the mesh is not increased by the presence of the reinforcement bar elements because an embedment technique is used to account for the increased stiffness of the backfill as a result of the presence of the layer(s) of reinforcement (see paragraph 29). The only restriction imposed by the embedment procedure is the number of individual bar elements created by SOILSTRUCT. A bar element is created for each solid element intersected by a reinforcement layer. At present, up to 500 bar elements can be created.

There are two restrictions regarding the layout of reinforcement layer(s); (1) the layers may not be coincident with the horizontal sides of any two-dimensional soil element, and (2) the layer(s) may not intersect any nodal point defining a triangular soil element. Where these restrictions might apply, the coordinates of the reinforcement and the element side/nodes need only differ by a very small amount ( $>10^{-5}$ ).

(a) **FIRST CARD**

<u>Variable</u>	<u>Explanation</u>
REBARS	Number of layers of reinforcement material.
BAR_STIF	Product of cross-sectional area and Young's moduli, (A·E), per unit width.

(b) **SECOND CARD**

<u>Variable</u>	<u>Explanation</u>
MATR_FILL(N)	Material type number for two-dimensional soil element containing reinforcement.  Additional material type numbers, N = 2 to R_FILL , are specified in the next columns and on additional cards as required.

(c) **THIRD CARD**

<u>Variable</u>	<u>Explanation</u>
J	Number of reinforcement layer.
XI(J)	X-coordinate of the left-most end of reinforcement layer J .
YI(J)	Y-coordinate of the left-most end of reinforcement layer J .
XJ(J)	X-coordinate of the right-most end of reinforcement layer J .
YJ(J)	Y-coordinate of the right-most end of reinforcement layer J .

This card is repeated for J = 2 to REBARS layers of reinforcement.

### 13. CONTINUATION OR INITIALIZATION CARDS

This input is supplied only if INIT = 0 , and is supplied from disc storage that has been generated during a preceding analysis. This option is provided so that a required sequence of loading steps can be stopped at an intermediate step, then restarted from that step without repeating the complete analysis. These cards may also be used to specify values for particular variable(s) in an initial analysis without using the gravity turn-on procedure. Similarly, values assigned to specific variables can be changed if the sequence of loading is stopped prior to a restart analysis.

(a) **FIRST CARD (ELEMENT INFORMATION) — FORMAT (4I5)**

<u>Column</u>	<u>Variable</u>	<u>Explanation</u>
1-5	NUMEL	Number of elements in the mesh, excluding bar elements, but including interface elements.
6-10	NUMJT	Number of interface elements.
11-15	NUMBAR	Number of bar elements, including those initially in the mesh and those added in previous loading steps (if a restart analysis).
16-20	NUMNP	Number of nodal points.

(b) **SECOND CARD (STRESS INFORMATION) — FORMAT (4F20.6)**

One card is supplied for each interface element or two-dimensional element, in numerical sequence  $N = 1$  to NUMEL .

<u>Column</u>	<u>Variable</u>	<u>Explanation</u>
1-20	SIG(N,1)	Stress in the x-direction for a two-dimensional element, $\sigma_x$ , normal stress for an interface element.
21-40	SIG(N,2)	Stress in the y-direction for a two-dimensional element, $\sigma_y$ , shear stress for an interface element.
41-60	SIG(N,3)	x-y shear stress for a two-dimensional element $\tau_{xy}$ , zero or blank for interface element.
61-80	SIG(N,4)	Maximum previous value of x-y shear stress for a two-dimensional element; zero or blank for interface element.

(c) **THIRD CARD (NODAL POINT INFORMATION) — FORMAT (2D15.9, 1F9.2, 2X, 2D15.9, 1F9.2)**

Information for two nodal points is supplied on each card. Nodal points are specified in numerical order,  $N = 1$  to NUMNP .

<u>Column</u>	<u>Variable</u>	<u>Explanation</u>
1-15	DISPX(N)	Displacement in x-direction.
16-30	DISPY(N)	Displacement in y-direction.
31-39	PP(N)	Pore pressure in head of water.
41-56	DISPX(N+1)	Displacement in x-direction.
57-71	DISPY(N+1)	Displacement in y-direction.
72-80	PP(N+1)	Pore pressure in head of water.

Information for the next two nodal points is supplied on subsequent lines.

(d) **FOURTH CARD (MATERIAL TYPE DESIGNATION) — FORMAT (15I5)**

Material type numbers for 15 two-dimensional or interface elements are specified on each card. Material type numbers for elements in numerical sequence, N = 1 to NUMEL , are specified.

<u>Column</u>	<u>Variable</u>	<u>Explanation</u>
1-5	IL(N,5)	Material type number.
		Material type numbers for the next 14 elements are supplied in the next 14 five-column fields.

Note that material type numbers supplied on these cards supersede the material type numbers specified on the element card (section 9). Thus material type changes can be made as part of a restart analysis rather than including such changes in a loading step of an analysis.

(e) **FIFTH CARD (BAR ELEMENT INFORMATION) — FORMAT (3I5,2D10.7, 2D10.1, D10.5)**

This card is supplied only if bar elements are included (NUMBAR > 0). Information for bar elements is specified on each card. Information is supplied for bar elements in numerical sequence, N = 1 to NUMBAR .

<u>Column</u>	<u>Variable</u>	<u>Explanation</u>
1-5	IB(N,1)	Number of nodal point I .
6-10	IB(N,2)	Number of nodal point J .
11-15	IB(N,3)	Spring response type code - = 1 if both compression and tension of bar allowed. = 2 if only compression allowed. = 3 if only tension allowed.
16-25	BAR(N,1)	$\cos \alpha$
26-35	BAR(N,2)	$\sin \alpha$
36-45	BAR(N,3)	Prestress force in the bar element.
46-55	BAR(N,4)	Stiffness of bar element, (AE/L).
56-65	BAR(N,5)	Displacement of bar element at activation.

Note that these parameters, if changed for a restart analysis, supersede those specified on the Bar Element Card (section 10). Also, if bar elements are initially included in the mesh, and this initialization procedure is used, then this card must be included, duplicating the information specified in the Bar Element Card.

(f) **SIXTH CARD (INTERFACE INFORMATION) — FORMAT (8D10.4)**

This card is supplied only if interface elements are included ( $NUMJT > 0$ ). Information for four interface elements is specified on each card. Information is supplied for interface elements in numerical sequence,  $N = 1$  to  $NUMJT$ .

<u>Column</u>	<u>Variable</u>	<u>Explanation</u>
1-10	STFS(N)	Shear stiffness of first interface element.
11-20	STFN(N)	Normal stiffness of first interface element.  Information for the next three interface elements is supplied in the next six 10-column fields.

Note that the value of the shear stiffness, if changed for a restart analysis, supersedes the value specified on the Interface Property Card (section 6). Thus the interface stiffness can be changed as part of a restart analysis.

(g) **SET OF 5 CARDS (REINFORCEMENT BAR INFORMATION)**

This set of 5 cards is supplied only if reinforcement bar elements are included ( $R\_FILL \neq 0$ ).

**Card 1 of 5 — FORMAT (I5)**

<u>Column</u>	<u>Variable</u>	<u>Explanation</u>
1-5	REBAR_NUM	Number of reinforcement bar elements.

**Card 2 of 5 — FORMAT (I5I5)**

<u>Column</u>	<u>Variable</u>	<u>Explanation</u>
1-5	EMBED(N,1)	Two-dimensional soil element number in which the reinforcement bar number $N$ is contained.  Information for $N = 1$ to $REBAR\_NUM$ reinforcement bar elements are to be provided. The next 14 $EMBED(N,1)$ values are supplied in the next 14 columns.

**Card 3 of 5 — FORMAT (1D15.9, 1025.19, 1D15.9, 1D25.19)**

<u>Column</u>	<u>Variable</u>	<u>Explanation</u>
1-15	R_COORD(N,1,1)	X coordinate for reinforcement bar element node I.
16-40	R_COORD(N,2,1)	Local X coordinate for reinforcement bar element node I.
41-55	R_COORD(N,1,2)	X coordinate for reinforcement bar element node J.
56-80	R_COORD(N,2,2)	Local X coordinate for reinforcement bar element node J.

There are  $REBAR\_NUM$  cards provided.

#### Card 4 of 5 — FORMAT (8D10.4)

<u>Column</u>	<u>Variable</u>	<u>Explanation</u>
1-10	STIF_TEMP(N)	Product of cross-sectional area and Young's moduli, (A·E) , per unit width for reinforcement bar element N .  Information for the next seven reinforcement bar elements is supplied in the next seven fields. There are REBAR_NUM values provided.

#### Card 5 of 5 — FORMAT (7D11.5)

<u>Column</u>	<u>Variable</u>	<u>Explanation</u>
1-11	R_FORCE(N,2)	Reinforcement bar element strain.  Information for the next six reinforcement elements is supplied in the next six fields. There are REBAR_NUM values provided.

### 14. LOADING STEP CARDS

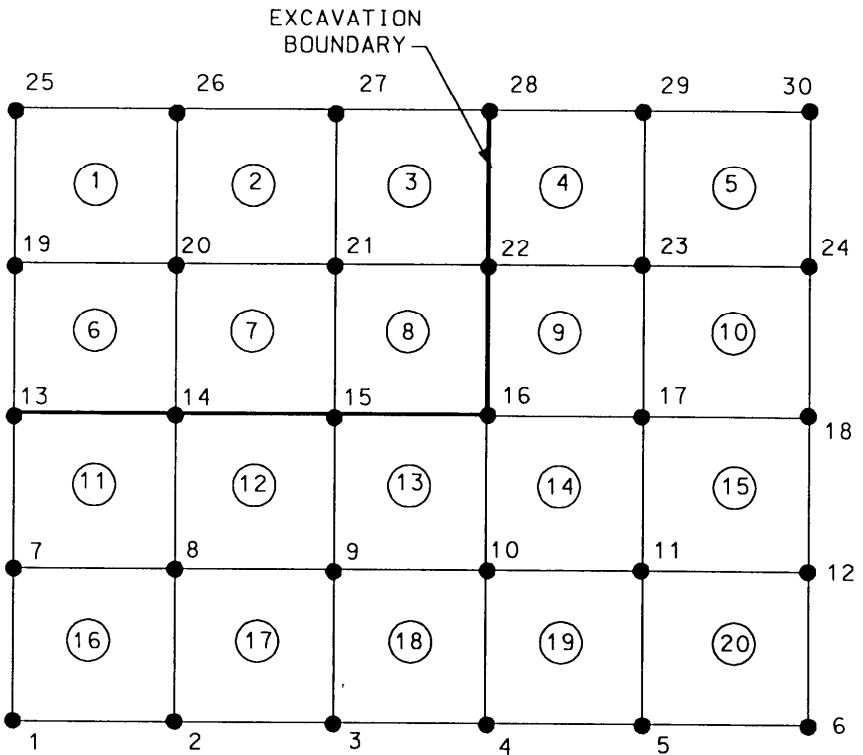
These cards are required only if the number of load steps is greater than zero,  $NC \neq 0$  . Up to three load/construction modes may be used per load step, as described in section 3. Cards are assembled in the order specified on the Loading Information Cards (section 3): cards for the first load/construction mode specified for the first loading step, and so on, to the cards for the last load/construction mode specified for the last construction step.

For a given loading step, the lowest numbered load/construction mode is processed first, but the analysis of the loading step is made for the combined effect of all load/construction modes specified for that loading step. Care must therefore be exercised in specifying some load/construction modes, such as material type changes or concentrated forces representing prestress forces, in the same loading step with other load/construction modes.

#### (a) EXCAVATION

These cards are supplied only if  $KCS(N,1)$  ,  $KCS(n,2)$  , or  $KCS(N,3) = 1$  . Input is handled by subroutine EXCAV . Free-excavated elements and common-excavated elements are input separately. A free-excavated element is an element specified to be excavated that has **no** boundary in common with an element not specified to be excavated in the loading step. A common-excavated element, therefore, has **at least one** boundary in common with an unexcavated element (Figure A4).

Interface elements can **only** be included as free-excavated elements, even if they have a boundary in common with an unexcavated element. Interface elements **cannot** be used as interpolation elements. Free-excavated elements (other than interpolation elements) can be used as interpolation elements, though common-excavated elements are more commonly used.



ELEMENTS 1 AND 2 ARE FREE EXCAVATED ELEMENTS.  
 ELEMENTS 3, 6, 7, AND 8 ARE COMMON EXCAVATED ELEMENTS.  
 NODES 13, 14, 15, 16, 22, AND 28 ARE LOADED BY EXCAVATION FORCES.  
 ELEMENTS 6, 7, AND 8 SHOULD BE INPUT SEQUENTIALLY FOR OPTIMUM EFFICIENCY.

*Figure A4. Example excavation load step defining free- and common-excavated elements in relation to the excavation boundary (Clough 1984)*

If possible, adjacent common-excavated elements should be input sequentially as this procedure avoids repetitive computation; nodal loads for a nodal point common to the two sequential elements will only be calculated once.

**(1) FIRST CARD (CONTROL DATA) — FORMAT (2I5)**

Column	Variable	Explanation
1-5	NFXEL	Number of free-excavated elements.
6-10	NXELCB	Number of common-excavated elements.

**(2) SECOND CARD (FREE-EXCAVATED ELEMENT DATA) — FORMAT (16I5)**

Element numbers of 16 free-excavated elements can be supplied on one card. A maximum of 150 can be specified in one loading step. Element numbers of all free excavated elements,  $N = 1$  to  $NFXEL$ , are to be specified.

Column	Variable	Explanation
1-5	LNCEL(N)	Element number of first free-excavated element. Information for the next 15 free-excavated elements is supplied in the next 15 five-column fields.

(3) **THIRD CARD (COMMON-EXCAVATED ELEMENT DATA) —  
FORMAT (8I5)**

One card is supplied for each common-excavated element,  $N = 1$  to  $NXELCB$ . A maximum of 150 common-excavated elements can be specified in one loading step.

Loading codes include:

- 0 - the node is not loaded by excavation forces, and is **not** common to both an excavated and an unexcavated element.
- 1 - the node is loaded by excavation forces and is common to both an excavated and an unexcavated element.

Notes I, J, K, and L refer to the same nodes I, J, K, and L specified on the element card (section 9).

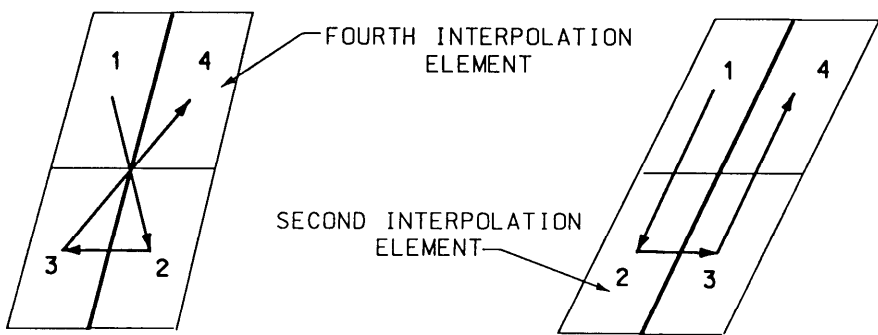
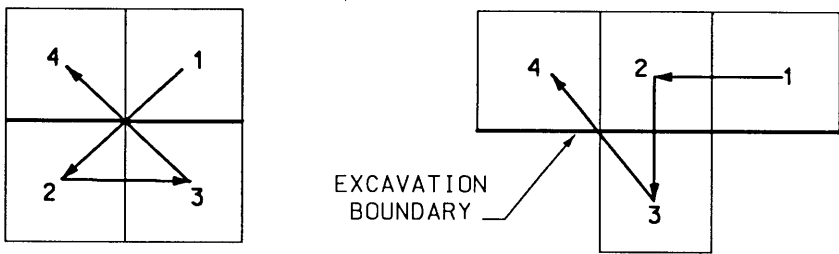
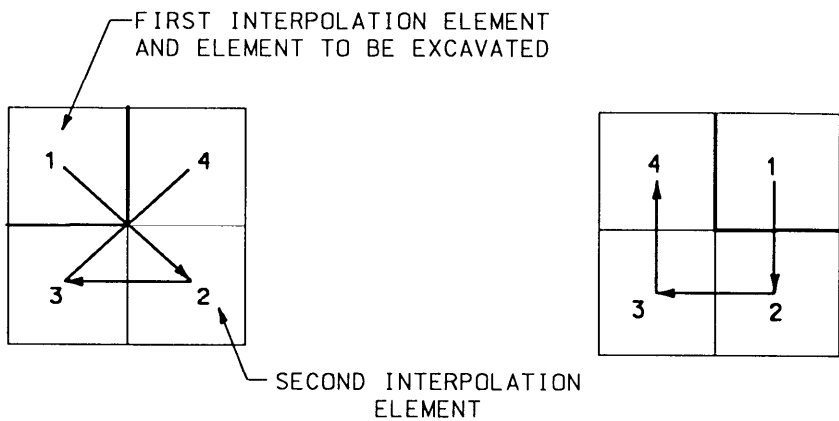
Interpolation elements should be specified in a crisscross fashion, as shown in Figure A5. Further, the x- or y-coordinates of diagonal elements must not be the same. If these rules are not adhered to, the interpolation routine will detect a singularity, and processing will stop.

Column	Variable	Explanation
1-5	LUL(N,1)	Element number of the first common-excavated element. This element is also the first interpolation element.
6-10	LUL(N,2)	Element number of second interpolation element.
11-15	LUL(N,3)	Element number of third interpolation element.
16-20	LUL(N,4)	Element number of fourth interpolation element.
21-25	LUL(N,5)	Loading code for node I.
26-30	LUL(N,6)	Loading code for node J.
31-35	LUL(N,7)	Loading code for node K.
36-40	LUL(N,8)	Loading code for node L.

Loading codes are specified for the nodes of the element to be excavated specified in columns 1-5.

(b) **FILL OR CONCRETE PLACEMENT**

These cards are supplied only if  $KCS(N,1)$ ,  $KCS(N,2)$ , or  $KCS(N,3) = 2$ . Input is handled by subroutine BUILD. The types of elements that can be placed include



a. ABOVE CONFIGURATIONS ARE ACCEPTABLE

b. ABOVE CONFIGURATIONS ARE NOT ACCEPTABLE

*Figure A5. Illustration of numbering of interpolation elements for calculation of stresses at the excavation boundary (Clough 1984)*

structural, soil, and interface elements. Subroutine SUBSTP cannot be used in conjunction with subroutine BUILD .

At placement, the fill element(s) is assigned a low modulus and the surface displacements are set equal to zero. Stresses assigned to the newly placed fill are based on  $\sigma_x = K_o \sigma_y$  or  $\sigma_x = \sigma_y$  (see KEYH20 on card group 2c), where  $\sigma_y$  is equal to the product of the unit weight of the fill element times the depth below the surface to the center of the element. If a fill element contains a reinforcement layer(s), then the bar element(s) representing the layer(s) will be added to the newly placed fill elements at the end of the load step. Generally, all fill elements associated with a particular layer should be added in one load step.

(1) **FIRST CARD (CONTROL DATA)** — FORMAT (2I5, D10.2, I5)

<u>Column</u>	<u>Variable</u>	<u>Explanation</u>
1-5	NLEL	Total number of elements to be placed, including interface and structure elements.
6-10	NONP	Number of nodal points within layer(s) to be assigned zero. This includes all nodal points for existing elements to be placed except points in common with an existing element.
11-20	HTB	New y-coordinate at the top of backfill.
21-25	NPANEL	Number of segment end points used to define the y-coordinates for the top of the backfill. NPANEL must be less than or equal to 30. If NPANEL = 0 , elevation of backfill = HTB value.

(2) **SECOND CARD (ELEMENT NUMBER)** — FORMAT (16I5)

Element numbers of 16 placed elements can be supplied on the card. A maximum of 250 can be specified in one loading step. Element numbers of all placed elements, N = 1 to NLEL , are to be supplied.

<u>Column</u>	<u>Variable</u>	<u>Explanation</u>
1-5	LEL(N,1)	Element number of first element to be placed.
6-10	LEL(N,2)	Material type number.  Information for the next seven place element numbers and their corresponding material types are supplied in the next 14 five-column fields.

(3) **THIRD CARD (NODE NUMBERS)** — FORMAT (16I5)

Nodal point numbers of 16 nodes to be assigned zero displacement can be supplied on one card. A maximum of 250 can be specified in one loading step. Nodal point numbers, N = 1 to NONP , are to be specified in sequential order.

<u>Column</u>	<u>Variable</u>	<u>Explanation</u>
1-5	NP(N)	Nodal point number of first node assigned zero displacement.  Information for the next 15 nodal points is supplied in the next 15 five-column fields.

**(4) FOURTH CARD (TOP OF BACKFILL) — FORMAT (2D10.2)**

<u>Column</u>	<u>Variable</u>	<u>Explanation</u>
1-10	XPANEL(N)	X-coordinate of ground surface segment end point.
11-20	YPANEL(N)	Elevation of ground surface at the segment end point.  Information for the remaining segment end points is supplied on subsequent cards.

**(c) SEEPAGE**

These cards are supplied only if  $KCS(N,1)$ ,  $KCS(N,2)$ , or  $KCS(N,3) = 3$ . Input is handled by subroutine SEEP. Seepage loads are determined from change in pore pressure specified as  $DP(N)$  on nodal point cards, or from the specified phreatic level changes.

**(1) FIRST CARD (CONTROL DATA) — FORMAT (I5)**

<u>Column</u>	<u>Variable</u>	<u>Explanation</u>
1-5	NCODE	Option code specifying how seepage loading data is to be input - = 0 if specified as $DP(N)$ on Nodal Point Card (section 7). = 1 if the seepage loading is to be calculated using the new phreatic surface input on the following cards.

**(2) SECOND CARD (NUMBER OF PHREATIC SEGMENTS) — FORMAT (I5)**

This card is required only if  $NCODE = 1$ .

<u>Column</u>	<u>Variable</u>	<u>Explanation</u>
1-5	NWAT	Number of phreatic surface segment end points used to specify the new phreatic surface. NWAT must be greater than or equal to 2. The number of phreatic surface segments is equal to NWAT. The maximum value of NWAT is 30.

**(3) THIRD CARD (PHREATIC LEVEL DATA) — FORMAT (6D10.2)**

This card is required only if  $NCODE = 1$ .

The end points of the phreatic surface segments delineating the new and old phreatic surfaces are specified as x-coordinates and must be the same as the x-coordinate of a nodal point (Figure A6). Both the present and new phreatic surfaces are assumed to be linear between the bounding x-coordinates. The left-hand side of the mesh is always the first bounding x-coordinate specified. A bounding x-coordinate on the old phreatic surface will require, usually, specification of the same x-coordinate on the new phreatic surface.

Two end points (x-coordinate), with associated new and old phreatic levels (y-coordinates), are supplied on each card. All end points,  $N = 1$  to  $NWAT$ , must be specified.

Column	Variable	Explanation
1-10	XW(N)	X-coordinate bounding the levels PREL(N) and FUEL(N) on the right-hand side. (Must) be the same as the x-coordinate of a nodal point.
11-20	PREL(N)	Present level (y-coordinate) of the phreatic surface at XW(N) .
21-30	FUEL(N)	New level (y-coordinate) of the phreatic surface at XW(N) .

Information for next end point is supplied in the next three 10-column fields.

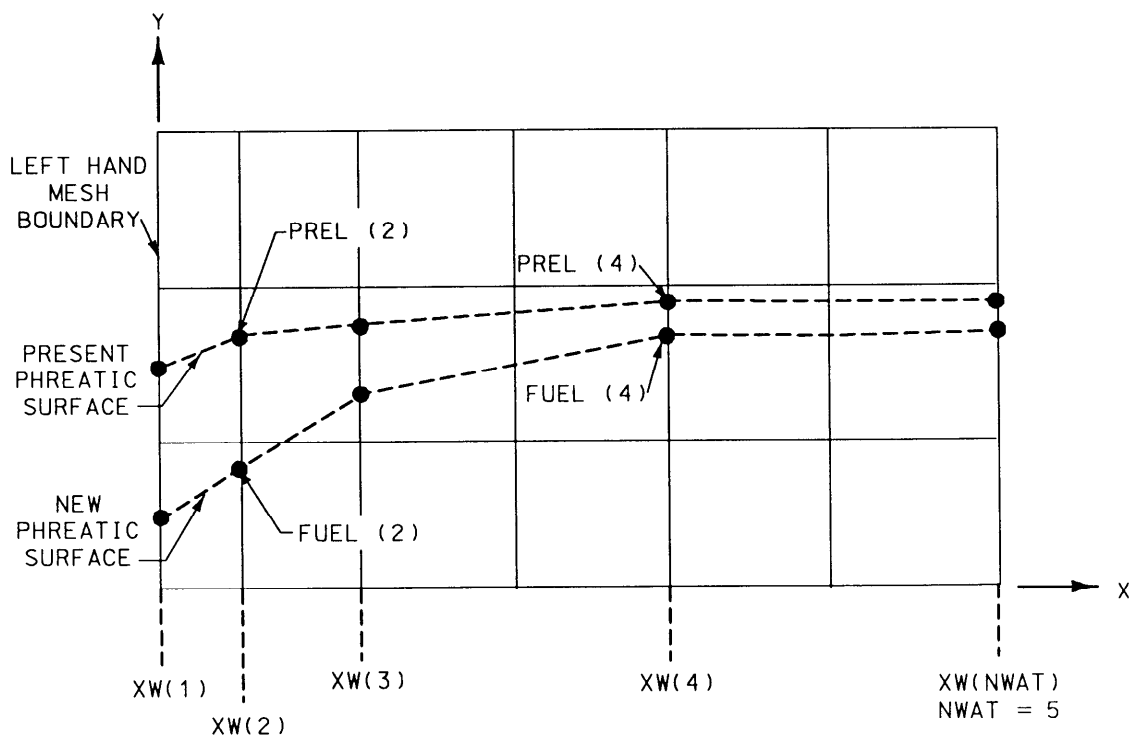


Figure A6. Example illustrating phreatic level data required for the seepage loading/construction case (Clough 1984)

#### (d) DELETION OF BAR ELEMENTS

These cards are supplied only if  $KCS(N,1)$  ,  $KCS(N,2)$  , or  $KCS(N,3) = 4$  . Input is handled by the main program.

The deleted bar elements remain in the mesh but with zero stiffness. The force the bar element carried is applied to the free node or nodes at its ends.

This loading/construction mode cannot be specified in the same loading step as fill or concrete placement.

##### (1) FIRST CARD (CONTROL DATA)

<u>Column</u>	<u>Variable</u>	<u>Explanation</u>
1-5	NCARDS	Number of deleted bar elements. There is no limit other than the number of bar elements presently in the mesh.

##### (2) SECOND CARD (ELEMENT NUMBERS)

The element numbers of 16 deleted bar elements can be specified on one card. A total of  $N = 1$  to NCARDS cards must be supplied.

<u>Column</u>	<u>Variable</u>	<u>Explanation</u>
1-5	N	Element number of bar element to be deleted.  Element numbers for the next 15 elements are supplied in the next 15 five-column fields.

#### (e) ADDITION OF BAR ELEMENTS

These cards are supplied only if  $KCS(N,1)$  ,  $KCS(N,2)$  , or  $KCS(N,3) = 5$  . Input is handled by the main program.

Information on the second card is the same as that explained for the Bar Element Card (Section 10). The added bar elements are numbered sequentially from  $NUMBAR + 1$  , where NUMBAR is the number of bar elements in the mesh before the present loading step.

##### (1) FIRST CARD (CONTROL DATA)

<u>Column</u>	<u>Variable</u>	<u>Explanation</u>
1-5	NCARDS	Number of bar elements to be added. Any number can be added in a loading step; however, the maximum number of bar elements that can be in the mesh (including inactive or deleted elements) is 15.

##### (2) SECOND CARD (ADDED BAR ELEMENT DATA)

<u>Variable</u>	<u>Explanation</u>
N	Element number of added bar element.
IB(N,1)	Number of nodal point I .

Variable	Explanation
IB(N,2)	Number of nodal point J .
IB(N,3)	Spring response type code.
BAR(N,1)	$\cos \alpha$
BAR(N,2)	$\sin \alpha$
BAR(N,3)	Prestress force in the bar element.
BAR(N,4)	Stiffness of bar element.
BAR(N,5)	Displacement of bar element at activation.

Note that in a restart analysis the added bar element(s) information must be included in the bar element connectivity cards (Section 10) and the value for NUMBAR in the data control card (Section 2a) must be updated.

#### (f) BOUNDARY PRESSURE LOADING

These cards are supplied only if  $KCS(N,1)$  ,  $KCS(N,2)$  , or  $KCS(N,3) = 6$  . Input is handled by subroutine SURFLD . Linear pressure distributions are assumed, based on the pressures specified for the nodal points.

##### (1) FIRST CARD (CONTROL DATA) — FORMAT (I5)

Column	Variable	Explanation
1-5	NLDS	Number of loaded boundaries.  There is no limit to the number of loaded boundaries that can be specified.
6-10	NOLDSX	Number of loaded boundaries for which the horizontal components of the nodal points load vectors are set equal to zero.
11-15	NOLDSY	Number of loaded boundaries for which the vertical components of the nodal points load vectors are set equal to zero.

##### (2) SECOND CARD (LOADED BOUNDARY DATA) — FORMAT (2I5, 4D10.2)

Information for one loaded boundary is specified on each card. Nodes I and J are specified counterclockwise on an element (Figure A7). A normal compressive traction (pressure) is positive. A tangential traction (shear stress) is positive **when directed clockwise (node J to node I) as shown in Figure A7**. A total of  $N = 1$  to  $(NLDS + NOLDSX + NOLDSY)$  loaded boundaries must be specified. NLDS cards are specified first, followed by NOLDSX cards and then NOLDSY cards.

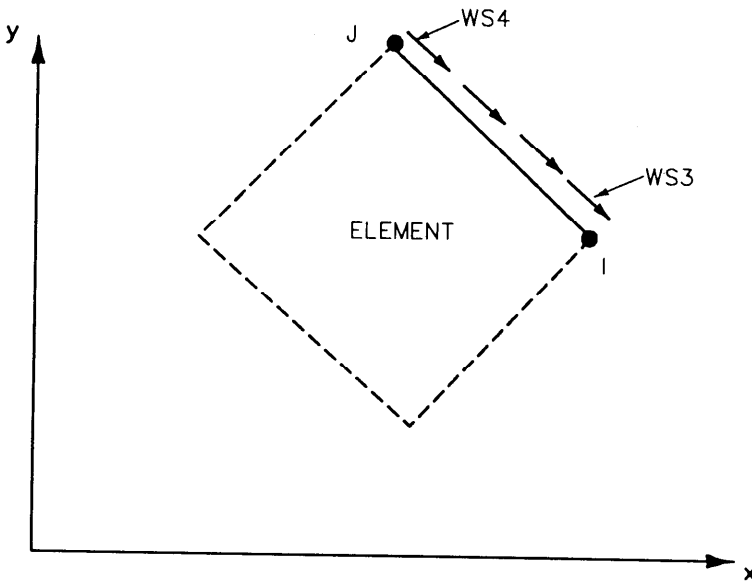
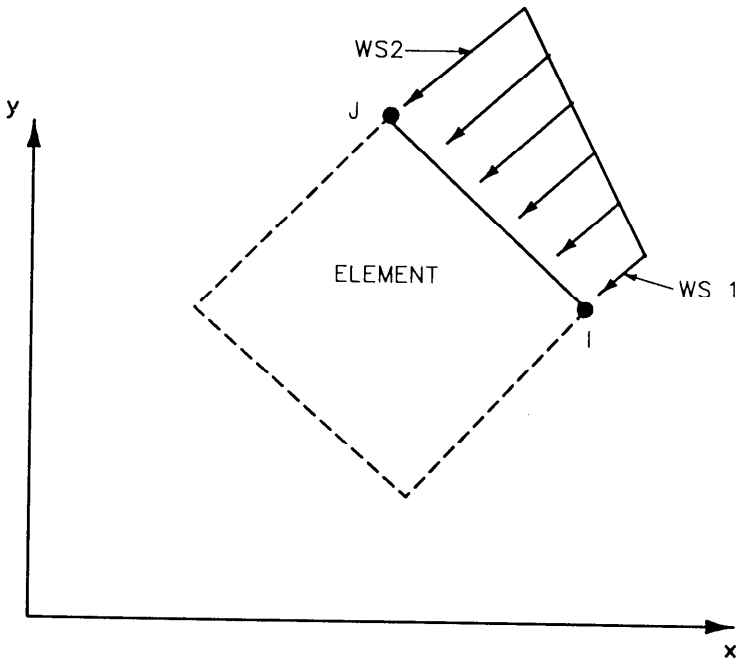


*Figure A7. Example of input parameters for positive boundary pressure loading*

<u>Column</u>	<u>Variable</u>	<u>Explanation</u>
1-5	I	Nodal point number of the first node of the loaded boundary.
6-10	J	Nodal point number of the second node of the loaded boundary.

<u>Column</u>	<u>Variable</u>	<u>Explanation</u>
11-20	WS1	Value of the normal pressure acting at node I .
21-30	WS2	Value of the normal pressure at node J .
31-40	WS3	Value of the shear stress acting at node I .
41-50	WS4	Value of the shear stress acting at node J .

**(g) TEMPERATURE LOADING**

**No cards are required** for this load/construction mode (Temperature Card, section 7). If  $KCS(N,1)$  ,  $KCS(N,2)$  , or  $KCS(N,3) = 7$  . Then the values of  $DP(N)$  are acknowledged by the main program and processed as temperature changes. Note that  $DP(N)$  can also be used to input phreatic level changes for the seepage loading/construction mode. Thus, if seepage is specified as being input through values of  $DP(N)$  , seepage and temperature loading cannot be included in the same loading step. Generally, temperature loading requires a restart analysis, with the  $DP(N)$  values being changed to reflect the temperature changes prior to the analysis.

The temperature scale used ( $^{\circ}C$  or  $^{\circ}F$ ) must correspond to the coefficient of thermal expansion designated on the Material Property Cards (Section 5). Temperature changes are typically designated for structural materials only.

**(h) CONCENTRATED FORCE OR DISPLACEMENT LOADING**

These cards are supplied only if  $KCS(N,1)$  ,  $KCS(N,2)$  , or  $KCS(N,3) = 8$  or  $9$  . Input is handled by the main program. Refer to the Loading Information Card (section 3) for instructions on using loading/construction modes 8 and 9.

**(1) FIRST CARD (CONTROL DATA)**

<u>Variable</u>	<u>Explanation</u>
NUMNDE	Number of loaded or displaced nodes. There is no limit to the number of loaded or displaced nodes that can be specified.

**(2) SECOND CARD (LOAD OR DISPLACEMENT DATA)**

Information for two loaded or displaced nodal points is supplied on each card. A total of  $N = 1$  to  $NUMNDE$  nodes must be specified. Sign convention is positive to the right (positive x-direction) and positive up (positive y-direction). Nodal points specified as being loaded or displaced **do not** have to be in numerical order.

<u>Variable</u>	<u>Explanation</u>
I	Node number of the first loaded or displaced node.
X1	Component of force or displacement in the x-direction at node I .
Y1	Component of force or displacement in the y-direction at node I .

<u>Variable</u>	<u>Explanation</u>
J	Node number of the second loaded or displaced node.
X2	Component of force or displacement in the x-direction at node J .
Y2	Component of force or displacement in the y-direction at node J .

Displaced nodes are to be included in Boundary Condition Cards (Section 8).

### (i) ELEMENT MATERIAL TYPE CHANGE

These cards are supplied only if  $KCS(N,1)$  ,  $KCS(N,2)$  , or  $KCS(N,3) = 10$  . Input is handled by the main program.

The material type of the specified element is changed **before** the analysis of the loading step which specifies the change. The material type change includes modifying the values of modulus  $E$  and Poisson's ratio  $G_{UI}$  and zeroing the stresses  $SIG(N,1)$  . Thus, if a material type change is specified in conjunction with boundary loading (in the same loading step) the elements whose material type is changed will respond to the loading with new material properties.

As included, this load/construction mode is intended to physically represent the grouting of an anchor. At a given step in the analysis, the material types of soil elements can be changed to represent the assumed linear elastic grout zone. If there is a need to change material types for any other reason, this can be done by stopping the analysis after the appropriate load step, modifying the material types on the material type designation card (Section 13d), then restarting the analysis.

#### (1) FIRST CARD (CONTROL CARD)

The maximum number of elements whose material type number can be changed in a load step is 150. The excavation and material type change loading/construction modes **cannot** be specified in the same loading step since the same variable,  $LUL(N,I)$  , is used to input data for both.

<u>Variable</u>	<u>Explanation</u>
NELCH	Number of elements whose material type number is being changed.

#### (2) SECOND CARD (ELEMENT DATA)

A total of  $N = 1$  to  $NELCH$  element numbers and new material type numbers must be specified.

<u>Variable</u>	<u>Explanation</u>
$LUL(N,7)$	Element number of first element with a specified new material type number.

<u>Variable</u>	<u>Explanation</u>
LUL(N,8)	<p>New material type number of the specified element.</p> <p>Information for the subsequent elements is supplied in the next columns and on additional cards as required.</p>

### **Output Data Sequence**

The input data read in the main program is printed out prior to the analysis of the first load step. Nodal point data, element data, and initial stresses are printed out only if specified. Loading/construction mode information for a load step is printed out prior to the analysis of the load step. Analysis results, excluding nodal displacement, can be specified to be printed out after each iteration or after the final iteration of each substep of a loading step. Continuation data for a restart analysis can be stored on disks (in a card image format), or punched on cards, after the final iteration of the analysis of the last substep of the last loading step. Nodal displacements can be stored on disks (in a card image format), or punched on cards, after the final iteration of the analysis of each substep of a loading step.

Results for all element types for all iterations, with the exception of the final iteration, are based on one-half the incremental stress being used to update the previous stress. Thus, they do not reflect the full effect of the applied loads. These values of stress are used to update modulus and stiffness values while iterating.

Different results, of course, are printed out for the different types of finite elements used. All output pages are identified by the analysis description. Headings designating the type of results (element-type), the load step number, the substep number, and the iteration number are included following the analysis description.

## 1. DISPLACEMENTS

Displacements for all nodes are printed out after the last iteration of each substep of a loading step.

<u>Column</u>	<u>Heading</u>	<u>Explanation</u>
1-10	NODAL POINT	Nodal point number.
11-18	X	X-coordinate of the node.
19-26	Y	Y-coordinate of the node.
27-40	TOTAL UX	Total displacement of the node in the X-direction.
41-54	TOTAL UY	Total displacement of the node in the Y-direction.
55-68	INCREM UX	Incremental displacement of the node in the X-direction.
69-82	INCREM UY	Incremental displacement of the node in the Y-direction.
83-93	PORE PRESS	Pore pressure acting on the node in the head of water.
94-100	NODAL POINT	Nodal point number.

## 2. RESULTS FOR TWO-DIMENSIONAL ELEMENTS

Results for two-dimensional elements are printed as requested using the input data described in section 2a. Elements numbered from  $N = (\text{NUMJT} + 1)$  to  $\text{NUMSOL}$  are included.

### (a) FIRST CARD: STRESSES & NEW MODULUS VALUES

<u>Column</u>	<u>Heading</u>	<u>Explanation</u>
2-5	ELE NO	Element number.
7-14	X	X-coordinate of element center.
16	E or T	Letter E indicating effective stresses output if a drained material or T indicating total stress output if an undrained material.
18-28	SIGMA X	Normal stress acting in the X-direction.
30-40	TAU XY	Shear stress acting in the X- and Y-directions.
42-52	SIGMA 1	Major principal stress.

<u>Column</u>	<u>Heading</u>	<u>Explanation</u>
54-60	THETA	Angle of the major principal plane, in degrees measured counterclockwise from the positive x-axis.
62-71	NEW E	New value for Young's moduli.
73-82	NEW B	New value for bulk moduli.
83-87	NEW NU	New value for Poisson's ratio.
88-94	PORE PRESS	Pore pressure.

(b) **SECOND CARD: STRESS VALUES AND OLD MODULUS VALUES**

<u>Column</u>	<u>Heading</u>	<u>Explanation</u>
7-14	Y	Y-coordinate of element center.
18-28	SIGMA Y	Normal stress acting in the Y-direction.
30-40	TAU MAX PREVIOUS	Maximum previous shear stress.
42-52	SIGMA 3	Minor principal stress.
54-60	STRESS RATIO	Stress level or ratio.
62-71	OLD E	Old value for Young's moduli.
73-82	OLD BULK	Old value for bulk moduli.
83-87	OLD NU	Old value for Poisson's ratio.

### 3. RESULTS FOR INTERFACE ELEMENTS

Results for interface elements are printed out following two-dimensional elements, as specified by ITRD . Elements numbered from N = 1 to NUMJT are included.

<u>Column</u>	<u>Heading</u>	<u>Explanation</u>
1-12	ELEM NO	Element number.
13-20	X	X-coordinate of element center.
21-28	Y	Y-coordinate of element center.
29-44	NORMAL STRESS	Normal stress acting on the element.
45-60	SHEAR STRESS	Shear stress acting on the element.
61-76	NORMAL STIFF	Normal stiffness.

<u>Column</u>	<u>Heading</u>	<u>Explanation</u>
77-92	SHEAR STIFF	Shear stiffness.
93-100	SL	Stress level.
101-112	PORE PRES	Pore pressure acting on the element.
113-122	ELEM NO	Element number.

#### 4. RESULTS FOR BAR ELEMENTS

Results for bar elements are printed following the results for the interface elements. Bar elements numbered from  $N = 1$  to NUMBAR are included.

<u>Column</u>	<u>Heading</u>	<u>Explanation</u>
1-13	BAR ELEM	Bar element number.
14-19	I	Nodal point number of the I node of the element.
20-25	J	Nodal point number of the J node of the element.
26-33	TYPE	Bar element response type code (see section 10 of the input listing).
34-47	COMPR	Force in the bar element (positive if compressive).
48-61	COMPRESSION	Change in length of the bar element (positive if compressive).
62-75	STIFFNESS	Stiffness of the bar element.
76-85	COSA	$\cos \alpha$ .
86-95	SINA	$\sin \alpha$ .
96-105	BAR ELEM	Bar element number.

#### 5. RESULTS FOR BAR ELEMENTS USED AS STRAIN GAGES

The results for bar elements used as strain gages are printed following the results for the bar elements. The bar elements numbered from  $N = 1$  to NSTRAN are included.

<u>Column</u>	<u>Heading</u>	<u>Explanation</u>
1-7	BAR ELEM	Element number for bar used as strain gage.
8-20	STRAIN	Strain in bar element.
21-35	BAR STRESS	Stress in steel at location of bar element used as a strain gage.
36-51	CONCRETE STRESS	Stress in concrete at location of bar element used as a strain gage.

## 6. RESULTS OF MOMENT COMPUTATIONS

The results for each pair of bar element strain gages used in the moment computations are printed following the results for the bar elements used as strain gages.

<u>Column</u>	<u>Heading</u>	<u>Explanation</u>
1-10	PAIR No.	Number of bar element strain gage pair.
11-20	X-CENTER	X-coordinate of center of member.
21-30	Y-CENTER	Y-coordinate of center of member.
31-45	GAGE No. 1	Bar element number for strain gage No. 1.
46-60	GAGE No. 2	Bar element number for strain gage No. 2.
61-70	$E_e$	Young's modulus of equivalent member.
71-80	$h_e$	Width of equivalent member.
81-95	$I_e$	Moment of inertia of equivalent member.
96-110	AXIAL FORCE	Resultant force acting normal to cross-section of equivalent member.
111-125	MOMENT	Moment at equivalent member.

## 7. RESULTS FOR REINFORCEMENT ELEMENTS

The results for bar elements used as soil reinforcement elements are printed following the moment computations.

<u>Column</u>	<u>Heading</u>	<u>Explanation</u>
1-4	BAR No.	Reinforcement bar element number.
5-13	ELM No.	Soil element number in which reinforcement bar element is embedded.
14-21	$X_i$	X-coordinate of bar node I.
22-34	$Y_i$	Y-coordinate of bar node I.
35-47	$X_j$	X-coordinate of bar node J.
48-60	$Y_j$	Y-coordinate of bar node J.
61-74	FORCE per WIDTH	Force in bar per unit width.
75-95	AREA · MODULUS	Product of cross-sectional area and Young's modulus.
96-111	STRAIN	Strain in bar.

## APPENDIX B: SEQUENCE OF OPERATIONS

1. The program SOILSTRUCT uses the direct stiffness method,  $\{F\} = [K]\{u\}$ , to solve for incremental nodal displacements  $\{u\}$  resulting from incremental loads applied to the nodal points  $\{F\}$ . The local element stiffness matrices are first formulated, then assembled into the global stiffness matrix. Equivalent nodal loads due to construction or applied loadings are assembled in the incremental load vector,  $\{F\}$ . The computed incremental displacements are then used to compute the incremental change in stress acting at the center of the elements. The values of total stress are updated by the computed incremental changes in stress. The total stresses are then used to revise the elastic moduli used in the formulation of the element stiffnesses. These procedures are repeated for each iteration, and in turn for each substep of each load case during the analysis. The determination of initial gravity stresses is accomplished in a similar fashion and can be viewed as an initial load step, with the nodal loads equal to the body forces.

2. The following is a listing of the names of each of the 26 subroutines comprising the program SOILSTRUCT and a brief description of their purpose:

- **Main Program.** The main program serves to control the execution of SOILSTRUCT. It calls subroutines, prints input data, load case information, material properties, node and element data, and boundary conditions. The input data for excavation, seepage, embankment construction, and boundary loadings are printed in their respective subroutines. Calculated equivalent nodal loads due to installation or deletion of bar elements, and concentrated forces or displacements, are added in the main program.
- **DETNA.** Subroutine DETNA calculates the number of degrees of freedom, determines the locations of the diagonal terms of the global stiffness matrix in the vector  $SN$ , and computes the required size of  $SN$ .
- **INITAL.** Subroutine INITAL calculates and prints initial stresses for a gravity turn-on analysis. This is done by sequential calls to STRSTF, OPTSOL, and STRESS. If a restart analysis is specified, INITAL reads the continuation data and initializes the material property, stress, and displacement arrays for the nodes and elements.
- **SUBSTP.** Subroutine SUBSTP controls the analysis of each load case when substeps are specified for that load case. SUBSTP divides the calculated equivalent nodal point loads, applied displacements, or temperature changes into the specified number of equal increments prior to performing the analysis.
- **STRSTF.** The terms of the global stiffness matrix are assembled in subroutine STRSTF by sequential calls to QUAD, JTSTF, and BAREL.
- **OPTSOL.** Subroutine OPTSOL solves the series of simultaneous equations using Crout reduction to obtain the incremental displacements.

- **STRESS.** Subroutine **STRESS** computes stresses and strains for the two-dimensional elements and prints the results. **STRESS** calls **MODCAL**, **BAREL**, and **JSTRES**, used to update the modulus values for two-dimensional elements, interface stiffnesses, and bar stiffnesses for use in the next iteration or load case.
- **QUAD.** Subroutine **QUAD** computes the local element stiffness matrix and stress-strain matrix for two-dimensional elements, computes equivalent nodal point forces due to temperature changes of non-soil elements, and computes equivalent nodal point forces due to gravity forces.
- **BAREL.** Subroutine **BAREL** computes the stiffness of the bar elements, and updates the bar forces.
- **JTSTF.** Subroutine **JTSTF** computes the stiffness of the interface elements.
- **JSTRES.** Subroutine **JSTRES** computes the stresses and relative displacements for the interface elements, updates the interface stiffness values, and prints results.
- **MODCAL.** Subroutine **MODCAL** updates the modulus values assigned to the soil elements.
- **BUILD.** Subroutine **BUILD** computes the nodal point loads which are equivalent to the weight of the elements representing a newly placed embankment lift and establishes the initial stresses and material properties for these newly placed elements.
- **EXCAV.** Subroutine **EXCAV** calculates the stresses acting on an excavation boundary.
- **EQNDFO.** Subroutine **EQNDFO** converts the stresses calculated by **EXCAV** to equivalent nodal point forces, which are added to the incremental load vector by **EXCAV**.
- **SURFLD.** Subroutine **SURFLD** computes equivalent nodal point forces due to a boundary pressure loading applied along the face of an element and adds these computed forces to the incremental load vector.
- **SEEP.** Subroutine **SEEP** calculates equivalent nodal point forces due to changes in the phreatic surface and adds these forces to the incremental load vector. The nodal point forces are formulated based upon changes in pore water pressures.
- **AUXOUT.** Subroutine **AUXOUT** writes continuation data to a file for use in subsequent analyses.
- **PRNCIP.** Subroutine **PRNCIP** calculates principal stresses and the maximum shear strain for two-dimensional elements.

- **PRNTFD.** All non-zero values of the incremental load vector are printed by subroutine PRNTFD.
- **GETFIL.** Subroutine GETFIL initializes the execution of SOILSTRUCT by requesting the names of the input and output files and the corresponding opening and closing of the disc storage devices.
- **CNVERT.** Subroutine CNVERT creates a disc storage file for use in the plotting of computed results by post-processors. Note that CNVERT discards all air elements and nodes attached only to air elements and renumbers the remaining existing nodes and elements.
- **REBAR.** The compilation of the arrays for the reinforcement bar elements is performed in subroutine REBAR.
- **FILLBARS.** Subroutine FILLBARS adds the reinforcement bar stiffnesses to the global stiffness array.
- **BARSTIF.** Subroutine BARSTIF computes the local reinforcement bar stiffness array.
- **RESTRESS.** Subroutine RESTRESS computes the reinforcement bar incremental strains and forces.
- **NFACTS.** Subroutine NFACTS computes the shape function for the reinforcement bar elements.

## APPENDIX C: BENDING OF STRUCTURAL MEMBERS

1. This appendix summarizes both simple beam theory and the theory of elasticity as applied to the bending of structural members. Simple beam theory is discussed in the first section, while the elastic response of flexural members bending in plane stress and plane strain are discussed in subsequent sections.

### Simple Beam Theory

2. Simple beam theory is the most elementary of the theories for flexural members. It relates the flexural displacements to stresses within a bending beam. Consider the bending response of the beam segment shown in Figure C1(a) when subjected to a moment of magnitude  $M$  (Figure C1(c)). In a pure bending problem, the resultant force acting along the  $x$ -axis equals zero. Simple beam theory assumes:

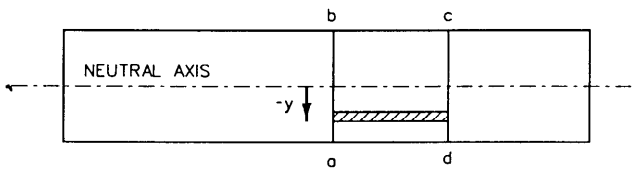
- a. The material comprising the beam is isotropic and homogenous.
- b. Transverse planes before bending remain transverse after bending; i.e., no shear distortions take place.
- c. The beam is a straight, prismatic member of constant cross section.
- d. The stress acting normal to the  $y$ -axis is zero.

The constant moment  $M$  causes the beam to deform in the manner shown in Figure C1(c); i.e., compression of the fibers along the top of the beam (the concave side) and extension of the fibers along the bottom of the beam (the convex side). The deformation of the beam will take the form of a circular arc of curvature  $\rho$ . Somewhere between the two sides, the beam fibers undergo no deformation. In this example, the  $x$ -axis is located so as to correspond to this plane and is referred to as the neutral axis. The length of the mid-plane beam segment  $abcd$  remains unchanged after flexure, equal to  $\Delta l$  (Figure C1(b) and Figure C1(d)). Due to the first assumption, the deformation varies linearly from the neutral axis to a maximum at the extreme fibers, as shown in Figure C1(d). The elongation  $\Delta u$  of the beam fibers at a distance equal to  $-y$  below the neutral axis is given by

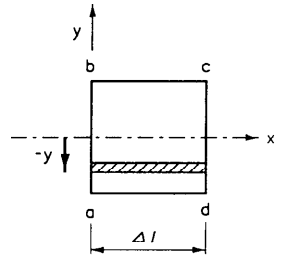
$$\Delta u = -y\Delta\theta \quad (C1)$$

with the change in length divided by the original length equal to

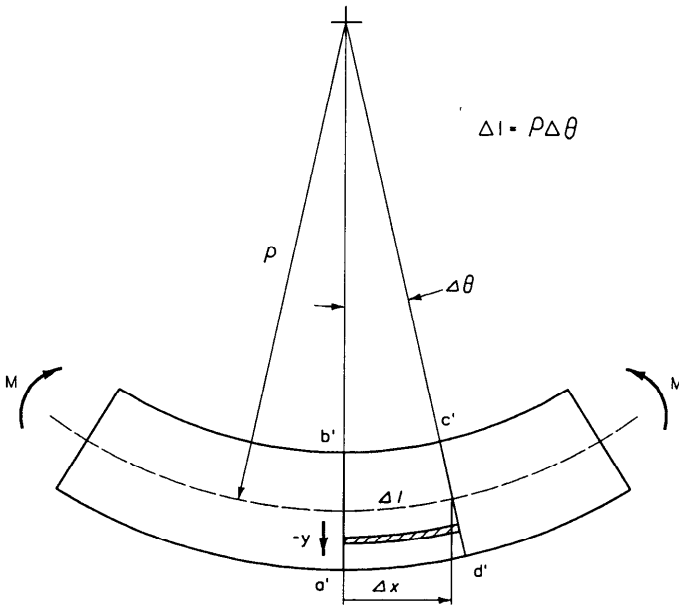
$$\frac{\Delta u}{\Delta l} = \frac{-y\Delta\theta}{\Delta l} \quad (C2)$$



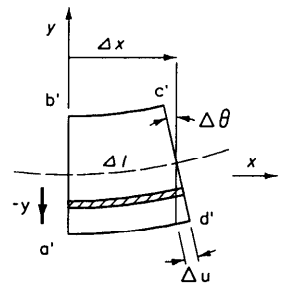
a.) Undeformed Beam Segment



b.) Undeformed Segment abcd



c.) Deformed Beam Segment



d.) Deformed Segment abcd

Figure C1. Deformation of a beam segment according to simple beam theory

The limit of Equation C2 as  $\Delta l$  approaches zero corresponds to  $du/dl$ , which is the linear tensile strain  $\epsilon_x$  in the beam fiber

$$\epsilon_x = \frac{du}{dl} \quad (C3)$$

at a distance  $-y$  from the neutral axis. Using the geometrical relationship  $\Delta l = \rho\Delta\theta$ , Equation C2, and considering the limit of the relationship as  $\Delta l$  approaches zero gives

$$\frac{1}{\rho} = -\frac{\epsilon_x}{y} \quad (C4)$$

For an elastic material the stress normal to the axis of bending is equal to

$$\sigma_x = E\epsilon_x \quad (C5)$$

The moment  $M$  is equal to

$$M = -\int_{\text{area}} \sigma_x y \, dA \quad (C6)$$

Introducing Equations C4 and C5 into C6 gives

$$M = \frac{E}{\rho} I \quad (C7)$$

where  $I$  is the moment of inertia of the cross-sectional area

$$I = \int_{\text{area}} y^2 \, dA \quad (C8)$$

Substituting Equations C4 and C5 into Equation C7 gives the flexure formula

$$\sigma_x = -\frac{My}{I} \quad (C9)$$

To summarize, the derivation of the flexure formula using simple beam theory assumes that the deformations within the beam are either the extension or compression of the beam fibers. This theory makes no assumptions regarding deformations in the y-axis direction nor in the out-of-plane direction. This fact contrasts with the response of a flexural member according to elastic theory, as described in the following two sections.

### Pure Bending of Beams in Plane Stress

3. The flexural response of beams bending in plane stress is developed in this section using the theory of elasticity. The generalized Hooke's Law for an isotropic, homogenous three-dimensional solid is expressed in tensor notation as

$$\epsilon_{ij} = \frac{1 + \nu}{E} \sigma_{ij} - \frac{\nu}{E} \delta_{ij} \sigma_{kk} \quad (C10)$$

where

$\epsilon_{ij}$  = the strain on the i plane in the j direction

$\sigma_{ij}$  = the stress on the i plane in the j direction

$\delta_{ij}$  = Kronecker delta (= 1 when i = j and = 0 otherwise)

$$\sigma_{kk} = \sigma_{11} + \sigma_{22} + \sigma_{33}$$

Hooke's Law may also be expressed as

$$\sigma_{ij} = \frac{E}{1 + \nu} \left[ \epsilon_{ij} + \frac{\nu}{1 - 2\nu} \delta_{ij} \epsilon_{kk} \right] \quad (C11)$$

where  $\epsilon_{kk} = \epsilon_{11} + \epsilon_{22} + \epsilon_{33}$ . In the case of pure bending of the Figure C2 prismatic beam in plane stress (the out-of-plane normal stress  $\sigma_{33} = 0$ ), bending stress results along the plane normal to the  $x_1$ -axis. In a plane stress problem, it is easily shown that the normal stress  $\sigma_{22}$  and the shear stresses  $\sigma_{12}$ ,  $\sigma_{13}$ , and  $\sigma_{23}$  are equal to zero, as well as the shear strains  $\epsilon_{12}$ ,  $\epsilon_{13}$ , and  $\epsilon_{23}$ . The bending stress  $\sigma_{11}$  is expressed as

$$\sigma_{11} = \frac{E}{1 + \nu} \left[ \frac{1 - \nu}{1 - 2\nu} \epsilon_{11} + \frac{\nu}{1 - 2\nu} (\epsilon_{22} + \epsilon_{33}) \right] \quad (C12)$$

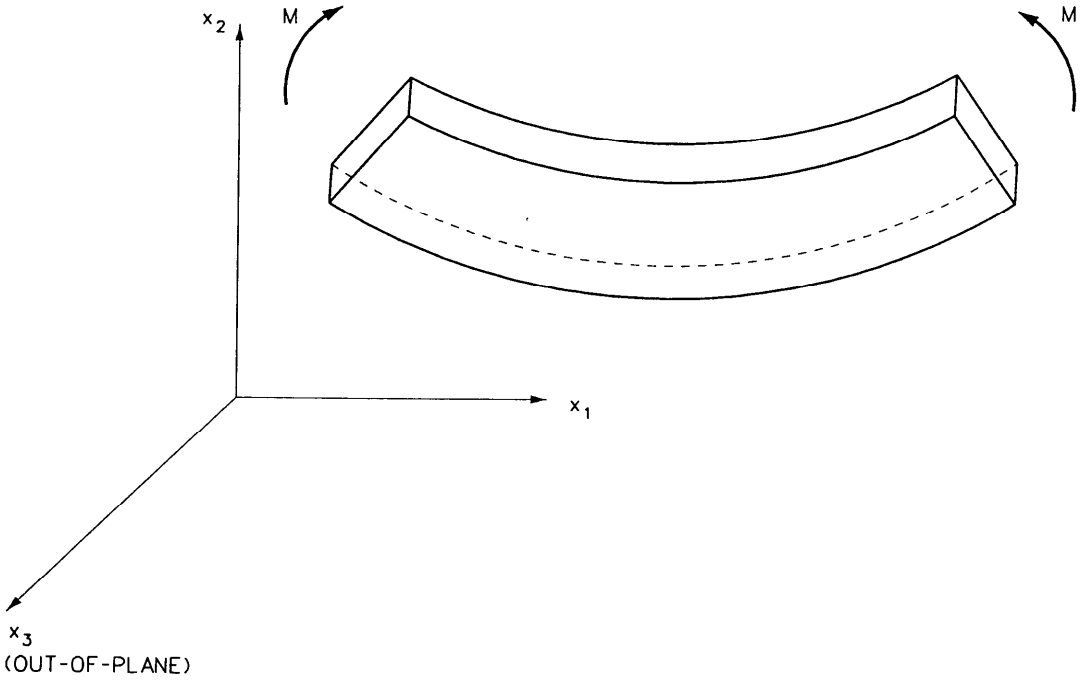


Figure C2. Pure bending of a prismatic beam in plane stress ( $\sigma_{33} = 0$ )

Equation C12 shows that strains normal to the  $x_2$ -axis and normal to the  $x_3$ -axis contribute to the value of the bending stress  $\sigma_{11}$  in contrast to simple beam theory. From Equation C10, the three normal strains are given by

$$\epsilon_{11} = \frac{1}{E} \sigma_{11} \quad (C13)$$

$$, \quad \epsilon_{22} = \frac{\nu}{E} \sigma_{11} \quad (C14)$$

and

$$\epsilon_{33} = \frac{\nu}{E} \sigma_{11} \quad (C15)$$

In the plane stress case, there are no restraints to movement in the  $x_2$  and  $x_3$  directions, and the strains normal to the  $x_2$ -axis and the  $x_3$ -axis are proportional to  $\epsilon_{11}$ .

$$\epsilon_{22} = -\nu \epsilon_{11} \quad (C16)$$

$$\epsilon_{33} = -\nu \epsilon_{11} \quad (C17)$$

Introducing Equations C16 and C17 into C12 results in the stress-strain relationship

$$\sigma_{11} = E \epsilon_{11} \quad (C18)$$

that is equivalent to the relationship for the bending stress from simple beam theory (Equation C9).

4. The flexural response of a bending member, modeled using a single row of solid finite elements, may be interpreted by using one-dimensional bar elements as strain gages. In this approach, as summarized in paragraph 43 for plane strain finite elements, bar elements are placed along the axis of bending, i.e. parallel to the  $x_1$ -axis, and located at the extreme fibers. Unlike simple beam theory, the  $\epsilon_{22}$  and  $\epsilon_{33}$  strains will contribute to the value of bending stress and therefore the corresponding stresses due to

bending in a displacement-based, plane stress finite element formulation. However, it has been shown in this section that the value for  $\sigma_{11}$  in a plane stress bending problem is equivalent to the bending stress from simple beam theory. It will be shown in the next section that this will not be the case when a plane strain finite element model is used.

### Pure Bending of Members in Plane Strain

5. The flexural response of structural members bending in plane strain is developed in this section using the theory of elasticity. In the case of pure bending of the Figure C3 long member in plane strain (the out-of-plane normal strain  $\epsilon_{33} = 0$ ), bending stresses result along the plane normal to the  $x_1$ -axis. In this problem, the normal stress  $\sigma_{22}$  is equal to zero, as well as all shear stresses and shear strains.  $\sigma_{33}$  is not equal to zero, unlike the plane stress problem. The bending stress  $\sigma_{11}$  is expressed as

$$\sigma_{11} = \frac{E}{(1 + \nu)(1 - 2\nu)} \left[ (1 - \nu)\epsilon_{11} + \nu\epsilon_{22} \right] \quad (C19)$$

The strain  $\epsilon_{22}$  can be removed from Equation C19 because, as for the plane stress case, there is no restraint to movement in the  $x_2$  direction. To accomplish this, the stress boundary conditions ( $\sigma_{22} = \sigma_{33} = 0$ ) are introduced to Equation C10. The resulting normal strains are given by

$$\epsilon_{11} = \frac{(1 + \nu)(1 - \nu)}{E} \sigma_{11} \quad (C20)$$

and

$$\epsilon_{22} = -\frac{(1 + \nu)\nu}{E} \sigma_{11} \quad (C21)$$

Strain normal to the  $x_2$ -axis, expressed in terms of the strain normal to the  $x_1$ -axis, is given by

$$\epsilon_{22} = -\frac{\nu}{1 - \nu} \epsilon_{11} \quad (C22)$$

By combining terms, Equation C20 becomes

$$\sigma_{11} = \frac{E}{(1 - \nu^2)} \epsilon_{11} \quad (C23)$$

By following the same steps described on page C3, the moment  $M$  is expressed as

$$M = -\frac{EI}{(1 - \nu^2)} \frac{\epsilon_{11}}{y} \quad (C24)$$

where  $y$  = distance from the neutral axis to the beam fiber at which the pure bending strain  $\epsilon_{11}$  is measured. Equation C23 differs from the relationship for bending stress

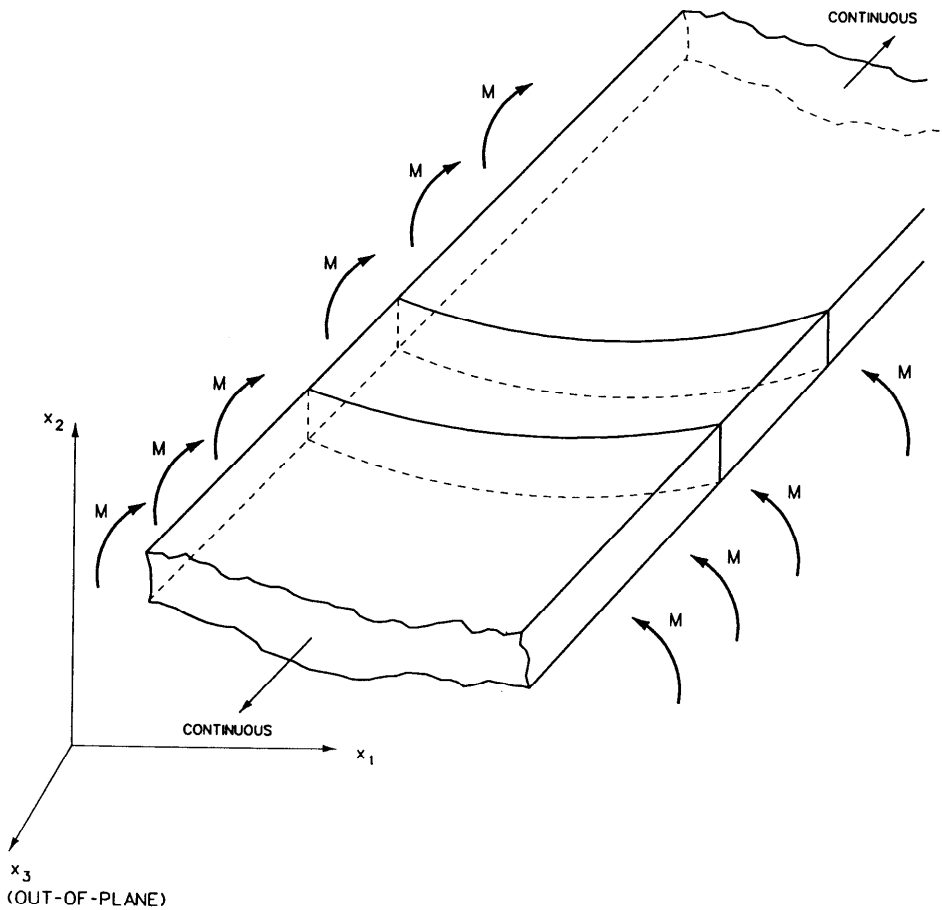


Figure C3. Pure bending of a long member inplane strain ( $\epsilon_{33} = 0$ )

in simple beam theory (Equation C9) by the factor  $1/(1 - \nu^2)$ . When a single row of solid finite elements are used to model the member bending in plane strain, one-dimensional bar elements are located along the axis of bending, i.e., parallel to the  $x_1$ -axis. The  $\epsilon_{22}$  strain will contribute to the value of bending stress and therefore the corresponding moment, as discussed in paragraph 42. Thus, when computing the internal moment that is equivalent to the  $\sigma_{11}$  distribution across the section, using the one-dimensional bar strains  $\epsilon_{11}$  from the plane strain finite element analysis, a factor equal to  $1/(1 - \nu^2)$  is included in the relationship (see Equation 31).

## APPENDIX D: NOTATION

$b_e$	Unit width of sheet-pile wall mesh
$B$	Bulk modulus
$c$	Cohesion intercept
$c_i$	Cohesion intercept for interface elements
$d$	Unit thickness of slice
$E$	Young's modulus
$E_e$	Equivalent Young's modulus
$E_i$	Initial Young's modulus
$E_t$	Tangent Young's modulus
$E_{ur}$	Young's modulus during unloading or reloading
$E_1$	Vertical stiffness
$E_2$	Hoop stiffness
[F]	Incremental load vector applied to the nodal points
$G_2$	Shear modulus
$H$	Vertical distance
$I$	Moment of inertia
$k_n$	Interface normal stiffness
$k_s$	Interface shear stiffness
$k_{si}$	Initial interface shear stiffness
$k_{st}$	Tangent interface shear stiffness
$K$	Modulus number
$\bar{K}$	Constant relating undrained Young's modulus to undrained strength
$\underline{K}$	Uniformly distributed radial spring acting to restrain radial movement
$K_b$	Bulk modulus
[ $K_b$ ]	Stiffness for reinforcement bar element
$K_j$	Interface modulus number
$K_o$	At-rest earth pressure coefficient
$K_s$	Planar spring stiffness
$K_{ur}$	Unload-reload modulus number

[K]	Global stiffness matrix
m	Bulk modulus exponent
M	Moment per unit width of wall
n	Modulus exponent
$n_i$	Interface modulus exponent
$\bar{p}$	Lateral pressure inside cell
$p'_c$	Effective consolidation pressure
P	Radial pressure inside cell
$P_a$	Atmospheric pressure
$r_c$	Radius of curvature for bending
R	Cell radius
$R_f$	Failure ratio
$R_{fi}$	Failure ratio for interface element
$S_u$	Undrained strength
SL	Stress level
$SL_i$	Stress level for interface element
T	Unit interlock force
$T_s$	Spring force
t	Cell-wall thickness
$\bar{t}$	Slice thickness (=1)
u	Node displacements, radial displacement of nodes
u	Incremental nodal displacements
$u_b$	Displacements of bar element nodes
$\Delta_n$	Nodal relative interface element displacements
$\Delta_s$	Average relative interface element shear displacements
$\Delta\sigma_1, \Delta\sigma_2, \Delta\sigma_3$	Changes in values of principal stress
$\delta$	Angle of interfacial friction along the interface
$\bar{\delta}$	lateral movement along the wall
$\epsilon_a$	Axial strain
$\epsilon_b$	Bending strain
$\epsilon_v$	Change in volumetric strain
$\epsilon_r, \epsilon_l$	Outer fiber strains

$\nu$	Poisson's ratio
$\nu_i$	Unfailed Poisson's ratio
$\gamma_w$	Unit weight of water
$\sigma_1$	Major principal stress
$\sigma'_1$	Major principal effective stress
$\sigma_3$	Minor principal stress
$\sigma'_3$	Minor principal effective stress
$\sigma'_h$	Horizontal effective stress
$\sigma'_v$	Vertical effective stress
$\sigma_n$	Normal stress
$\sigma_t$	Tensile strength
$(\sigma_1 - \sigma_3)$	Current deviator stress
$(\sigma_1 - \sigma_3)_f$	Deviator stress at failure
$(\sigma_1 - \sigma_3)_{ult}$	Ultimate deviator stress
$\tau$	Shear stress - interface element
$\tau_f$	Shear stress at failure - interface element
$\tau_{ult}$	Ultimate shear stress - interface element
$\phi$	Angle of internal friction